

# TVDiag: A Task-oriented and View-invariant Failure Diagnosis Framework with Multimodal Data

SHUAIYU XIE, Wuhan University, China

JIAN WANG\*, Wuhan University, China

HANBIN HE, Wuhan University, China

ZHIHAO WANG, Wuhan University, China

YUQI ZHAO, Central China Normal University, China

NENG ZHANG, SUN Yat-sen University, China

BING LI\*, Wuhan University, China

Microservice-based systems often suffer from reliability issues due to their intricate interactions and expanding scale. With the rapid growth of observability techniques, various methods have been proposed to achieve failure diagnosis, including root cause localization and failure type identification, by leveraging diverse monitoring data such as logs, metrics, or traces. However, traditional failure diagnosis methods that use single-modal data can hardly cover all failure scenarios due to the restricted information. Several failure diagnosis methods have been recently proposed to integrate multimodal data based on deep learning. These methods, however, tend to combine modalities indiscriminately and treat them equally in failure diagnosis, ignoring the relationship between specific modalities and different diagnostic tasks. This oversight hinders the effective utilization of the unique advantages offered by each modality. To address the limitation, we propose *TVDiag*, a multimodal failure diagnosis framework for locating culprit microservice instances and identifying their failure types (e.g., Net-packets Corruption) in microservice-based systems. *TVDiag* employs task-oriented learning to enhance the potential advantages of each modality and establishes cross-modal associations based on contrastive learning to extract view-invariant failure information. Furthermore, we develop a graph-level data augmentation strategy that randomly inactivates the observability of some normal microservice instances during training to mitigate the shortage of training data. Experimental results show that *TVDiag* outperforms state-of-the-art methods in multimodal failure diagnosis, achieving at least a 55.94% higher *HR@1* accuracy and over a 4.08% increase in F1-score across two datasets.

CCS Concepts: • Software and its engineering → Software maintenance tools.

Additional Key Words and Phrases: microservice-based system, multimodal data, root cause localization, failure type identification

## ACM Reference Format:

Shuaiyu Xie, Jian Wang\*, Hanbin He, Zhihao Wang, Yuqi Zhao, Neng Zhang, and Bing Li\*. 2024. TVDiag: A Task-oriented and View-invariant Failure Diagnosis Framework with Multimodal Data. 1, 1 (July 2024), 30 pages. <https://doi.org/XXXXXX.XXXXXXX>

---

\*Jian Wang and Bing Li are the corresponding authors of this paper. Authors' addresses: Shuaiyu Xie, theory@whu.edu.cn, Wuhan University, China; Jian Wang, jianwang@whu.edu.cn, Wuhan University, China; Hanbin He, hbsgsh@whu.edu.cn, Wuhan University, China; Zhihao Wang, zhihao\_wang@whu.edu.cn, Wuhan University, China; Yuqi Zhao, yuqizhao@ccnu.edu.cn, Central China Normal University, China; Neng Zhang, zhangn279@mail.sysu.edu.cn, SUN Yat-sen University, China; Bing Li, bingli@whu.edu.cn, Wuhan University, China.

---

Permission to make digital or hard copies of all or part of this work for personal or classroom use is granted without fee provided that copies are not made or distributed for profit or commercial advantage and that copies bear this notice and the full citation on the first page. Copyrights for components of this work owned by others than the author(s) must be honored. Abstracting with credit is permitted. To copy otherwise, or republish, to post on servers or to redistribute to lists, requires prior specific permission and/or a fee. Request permissions from permissions@acm.org.

© 2024 Copyright held by the owner/author(s). Publication rights licensed to ACM.

ACM XXXX-XXXX/2024/7-ART

<https://doi.org/XXXXXX.XXXXXXX>

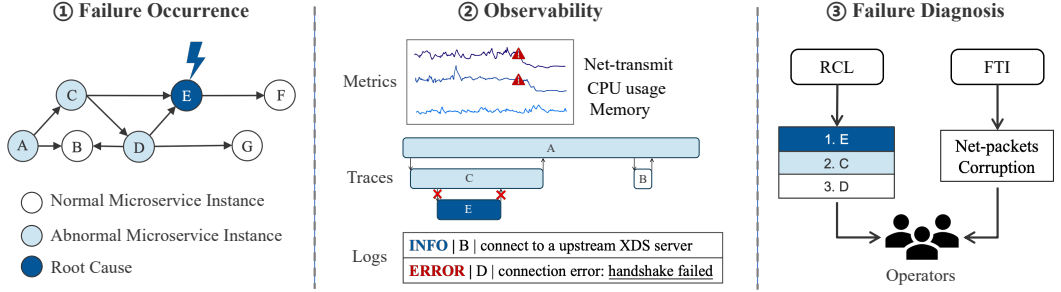


Fig. 1. An example of failure diagnosis in a microservice-based system. The network packets of microservice instance  $E$  are damaged, causing a failure in the system.

## 1 INTRODUCTION

Microservice architecture is gaining popularity in developing online systems because of its advantages of lower coupling, better resilience, and faster delivery. However, microservice-based systems frequently encounter reliability issues arising from their intricate interactions and expanding scale. For example, a failure in one microservice instance can propagate to other instances through message interactions between microservices, resulting in multiple instances becoming abnormal simultaneously [45], [47], [54]. The abundance of abnormal microservice instances has turned the root cause localization into a labor-intensive and error-prone endeavor. Operators may also struggle with identifying numerous suspected failure types (e.g., out-of-memory, network exception, and I/O pressure), leading to significant time consumption in selecting appropriate recovery strategies. Consequently, it is imperative to devise an automated diagnosis tool to enhance operators' efficiency and reliability in failure mitigation.

**Root Cause Localization (RCL)** and **Failure Type Identification (FTI)** are two fundamental tasks in failure diagnosis for microservice-based systems. RCL involves identifying the specific microservice instance responsible for the failure of a group of abnormal candidates. In contrast, FTI determines the type of the current failure, facilitating the selection of appropriate recovery measures. The growing observability of microservice-based systems allows for the utilization of multimodal monitoring data, including traces, logs, and metrics, to provide comprehensive insights into the status of microservice systems from various perspectives. More details of multimodal monitoring data can be found in Section § 2.2. Fig. 1 illustrates the two failure diagnosis tasks in a microservice-based system. Operators typically combine domain knowledge with the analysis of monitoring data, listing potential culprit microservices instances (i.e., RCL) and the failure type that may have triggered the incident (i.e., FTI). Current approaches primarily concentrate on diagnosing failures using single-modal monitoring data, which have progressed in specific diagnosis tasks. For example, log-based methods focus on mining event patterns and transforming them into rules to classify failure types [1, 2, 9, 12, 19, 26, 44, 49]. Trace-based methods, aided by rich dependency information, build system correlation graphs and simulate the failure propagation to infer root causes [15, 27, 28, 41, 48, 62, 65, 72]. Metric-based methods extract features of historical metrics to diagnose failures [6, 20, 30, 32, 35, 38–40, 50, 56–58, 70].

Despite the success of single-modal failure diagnosis methods in many scenarios, some specific failures are difficult to identify using a single modality due to the limited information each modality provides [64]. For instance, trace-based methods fall short in diagnosing hardware failures in the absence of fine-grained machine metrics [23]. As an example, we can find the error call (i.e.,  $C \rightarrow E$ ) based on the traces in Fig. 1, but we cannot ascertain the failure type (i.e., Net-packets Corruption)

solely based on the provided traces. This is because many failure types can cause error calls, such as unavailable service, server-side exception, or Net-packets Corruption. Meanwhile, metrics and logs can furnish macroscopic clues (i.e., sudden drop in net transmission and handshake failed) about this failure type. Although metrics and logs encapsulate more detailed information, they provide only local information about a microservice or a host, necessitating additional expertise to establish causal relationships for the entire system.

Given the limitations of single-modal failure diagnosis, several multimodal failure diagnosis methods based on deep learning have been proposed to integrate diverse data sources for different diagnosis tasks. DiagFusion [68] adopts an early fusion approach to convert multimodal data into event features uniformly during data processing. Eadro [23] intermediately fuses the high-dimensional features of each modality during model learning. Compared to single-modal failure diagnosis methods, these multimodal methods achieve significant performance improvements by combining complementary information from multiple views. Nevertheless, direct fusion is insufficient for extracting shared information among modalities, such as the system status and the abnormal microservice set. Furthermore, these methods often ignore the relationship between diagnosis tasks and modalities. In reality, the extent of contribution from various modalities tends to differ across specific diagnosis tasks. For instance, in RCL, operators typically need to construct the propagation path of a failure in a microservice-based system and then trace it back to locate root causes. This process involves building a correlation graph between microservices based on traces. In contrast, for FTI, log messages contain extensive descriptions of failure behaviors, such as *handshake failed* in Fig. 1, which effectively contribute to FTI. Therefore, tailoring diagnosis to task preferences can maximize the contribution of each modality.

This paper presents *TVDiag*, a multimodal failure diagnosis framework designed to locate root causes and identify failure types in microservice-based systems. For each failure, we apply alert detection for multimodal data of each microservice instance and then aggregate this alert information using a graph neural network. We then perform multi-task learning for RCL and FTI, leveraging the common knowledge to enhance the learning of each task. In this phase, we integrate three components with prior knowledge to guide *TVDiag* in leveraging the advantages of each modality and capturing shared information between them. The three components are described as follows:

- (1) **Task-oriented learning:** Considering the preference of a task for specific modalities, we introduce a novel task-oriented feature learning method to enhance the potential contribution of each modality to corresponding tasks.
- (2) **Cross-modal association:** As the multimodal data of a failure can be considered representations from distinct perspectives, some view-invariant information for the failure is shared across all modalities. We design a cross-modal association method based on contrastive learning [7] to capture this view-invariance information.
- (3) **Graph augmentation:** To mitigate the issue of insufficient labeled data and simulate failures with imperfect observability, we develop a graph-based data augmentation strategy by randomly inactivating non-root cause instances.

We conduct extensive experiments on two open-source multimodal datasets to evaluate the performance of *TVDiag*. Remarkably, *TVDiag* outperforms the state-of-the-art methods by 55.94% in *HR@1* accuracy for root cause localization and improves the F1-score by 4.08% for failure type identification. The main contributions are summarized as follows:

- We propose *TVDiag*, a multimodal failure diagnosis framework that locates root causes and identifies failure types in microservice-based systems. *TVDiag* integrates a task-oriented learning method to amplify the potential advantages of specific modalities in failure diagnosis.

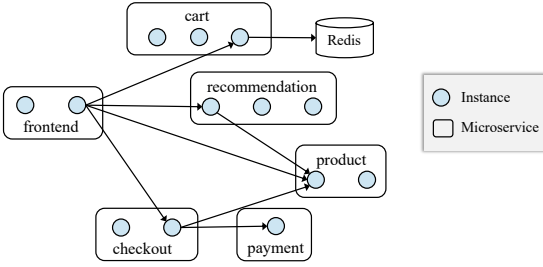


Fig. 2. Part of correlation graph in Online Boutique [13].

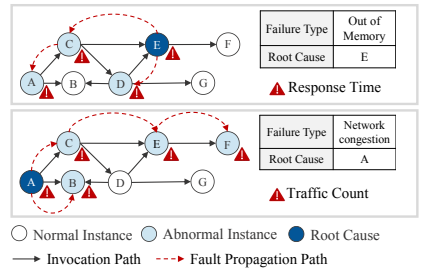


Fig. 3. Two examples of failure propagation.

Furthermore, *TVDiag* extracts view-invariant failure information shared across multimodal data based on cross-modal associations.

- We introduce a graph-based data augmentation strategy that involves random inactivation of non-root cause instances, thereby alleviating the problem of insufficient training data. This strategy can be easily integrated into existing frameworks without altering the primary network structure.
- We evaluate our framework using two open multimodal datasets, achieving substantial improvement across various metrics. The source code and experimental data are publicly available [52].

The rest of the paper is organized as follows. In Section 2, we provide an overview of the basic preliminaries in microservice-based systems and define the problem to be addressed in the paper. Section 3 delineates the motivation for using multimodal data. Furthermore, we offer insights into the preferences and view-invariance characteristics exhibited within multimodal data. In Section 4, we present a comprehensive description of our system. Section 5 details the evaluation metrics and presents the experimental results obtained. Section 6 offers the related work about failure diagnosis. The conclusion and future work are discussed in Section 7.

## 2 BACKGROUND

### 2.1 Microservice Architecture and Failure

**Microservice and Instance.** Microservice architecture aims to achieve lower coupling and faster delivery by breaking down a monolithic application into several independent microservices, each handling specific business tasks autonomously and communicating with one another [25, 45, 60]. To handle high volumes of incoming requests, each microservice typically runs a group of functionally identical instances, which act as workers processing specific business tasks. Fig. 2 illustrates a partial internal architecture of Online Boutique [13], a microservice-based e-commerce system developed by Google, highlighting the relationship between microservices and instance affiliation. When a user initiates a request to purchase a product in this system, the request will be received by a specific instance of the *frontend* microservice and then forwarded to instances belonging to other microservices. Although instances affiliated with a microservice undertake the same business task, their performance can vary significantly due to discrepancies in deployment environments and received traffic. Our focus is on locating the instance-level root cause, as identifying the microservice-level root cause can confuse operators due to the presence of numerous candidate instances.

**Failure.** A failure is characterized as the accumulation of multiple anomalies, which can lead to degraded system performance or even system unresponsiveness. According to MEPFL [72], failures are categorized into four broad categories: monolithic, multi-instance, configuration, and

asynchronous interaction. Typical examples of such failures include out-of-memory, network congestion, and process exits.

In a microservice-based system, a single failure in an instance can propagate to other instances due to frequent and intricate communication between microservices. Unfortunately, the trajectories and directions of failure propagation are often diverse and unpredictable [59]. Fig. 3 depicts two failure propagation scenarios in microservice-based systems. In the upper part, an out-of-memory malfunction causes a suboptimal performance for  $E$ , subsequently affecting its upstream instances waiting for its response. In the bottom part of Fig. 3, network congestion significantly reduces the transmission of network packages from instance  $A$ , leading to anomalous traffic counts in downstream instances. Both situations give rise to numerous anomalous instances and suspicious propagation trajectories. Although experienced operators can diagnose noticeable failures in one instance, failure propagation between instances complicates this process and impedes quick system recovery. Li et al. [30] also observed that most failures in online systems are recurring, meaning they repeatedly occur in different locations within microservice-based systems. Therefore, summarizing historical experiences and extracting failure fingerprints is essential for accurately diagnosing failures and implementing appropriate recovery measures.

## 2.2 Observability

Observability refers to the ability to measure the internal state of a system through monitoring data [37]. As illustrated in Section 1, the monitoring data is typically composed of three types: metrics, logs, and traces. These multimodal data sources have specific data structures and provide insights into microservice-based systems from different perspectives.

- **Traces.** Traces capture the execution path of each user request and record the information of all instances on that pathway. As shown in Fig. 4, a trace can be regarded as a tree, where each node records information related to an instance. A node is also called a span. Each span contains context (e.g., trace ID and span ID) and attributes (e.g., service name and instance name). Moreover, spans record the status of instances (e.g., start time, end time, and status code). For the sake of simplicity, we use the instance name to represent each span in all figures.
- **Metrics.** Metrics record the trends of system status and business performance in the form of time series. Generally, metrics are collected at fixed intervals and stored in numerical form. Fig. 4 lists three metrics related to system resource usage, recorded at one-minute intervals.
- **Logs.** Logs document events at different levels for each instance in a semi-structured text format. Logs typically consist of three elements: timestamps, log levels (e.g., INFO, WARN, and ERROR), and messages. Fig. 4 depicts three types of INFO-level logs and two types of ERROR-level logs. We can initially judge the severity of an event based on its log level and analyze the message to further understand the event's context and consequences. For example, the message of the first ERROR-level log indicates that a nonexistent user was queried in the database, while the second ERROR-level log relates to a MySQL connection failure. As such, logs, especially ERROR-level logs, have superiority in determining failure types.

Despite the usefulness of these modalities, operators face considerable challenges in diagnosing failures because of the heterogeneity of these data sources and the interference of large volumes of irrelevant data [3].

## 2.3 Problem Statement

Our work aims to pinpoint the root cause and classify the failure type based on multimodal monitoring data once a failure is detected. Hence, we must address two interconnected problems: **Root Cause Localization** (RCL) and **Failure Type Identification** (FTI). Failure diagnosis can

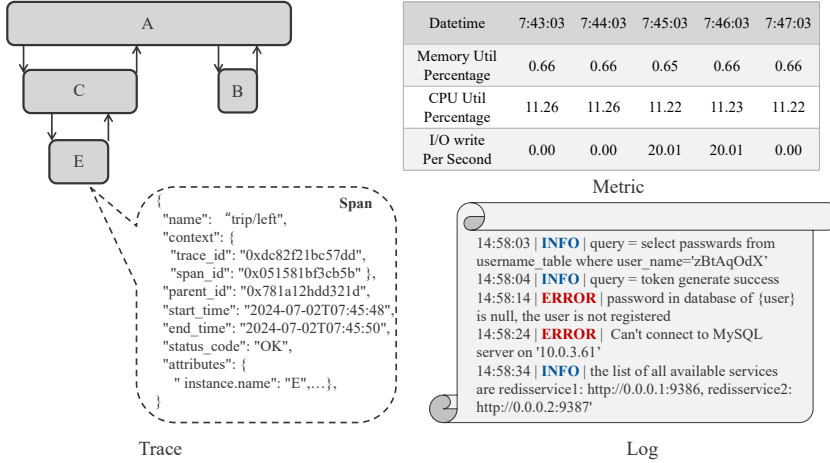


Fig. 4. Examples of data structures for three types of monitoring data.

assist operators in maintaining the reliability of the online system. As depicted in Fig. 1, RCL results in a ranking list  $\{E, C, D, \dots\}$  in descending order, enabling operators to identify the root cause instance  $E$  within a narrowed scope. Regarding FTI, we treat this task as a classification problem and categorize the current failure into a specific type, such as out-of-memory, facilitating the development of appropriate recovery measures (e.g., allocating more memory to instance  $E$ ).

Given the captured traces  $\mathcal{T}$ , system metrics  $\mathcal{M}$ , and collected logs  $\mathcal{L}$  of all instances over a period of time, we are committed to designing an automated diagnostic tool  $\mathcal{D}$  that identifies the underlying failure type  $t$  and ranks the culprit instances  $\mathcal{R}$ . We formulate our diagnosis process as:

$$\mathcal{D}(\mathcal{M}, \mathcal{T}, \mathcal{L}, \Theta) \rightarrow t, \mathcal{R}, \quad (1)$$

where  $\Theta$  represents the learnable parameters of  $\mathcal{D}$ .

### 3 MOTIVATION

To gain a deeper understanding of the impact of various monitoring data on failure diagnosis, we deployed Online Boutique [13] and deliberately injected multiple typical failures into its environment. Traces were collected by the Jaeger platform<sup>1</sup>, metrics were gathered using Prometheus<sup>2</sup>, and logs were sourced from the corresponding file system.

#### 3.1 The Necessity of Using Multimodal Data

Failure types in microservice-based systems are diverse and complex, ranging from insufficient external hardware resources to defects in the execution logic of a microservice. As mentioned in Section 1, any single-modal diagnosis method can hardly cover all failure scenarios due to the limited information offered by a single modality. To illustrate this point, we intentionally dropped some network packets received by one instance (named *product-1*) of the *product* microservice in Fig. 2. In this scenario, *product-1* is identified as the root cause, while Net-packets-loss represents the corresponding failure type. Fig. 5 shows real samples of multimodal monitoring data captured within a specific time window.

<sup>1</sup><https://www.jaegertracing.io/>

<sup>2</sup><https://prometheus.io/>

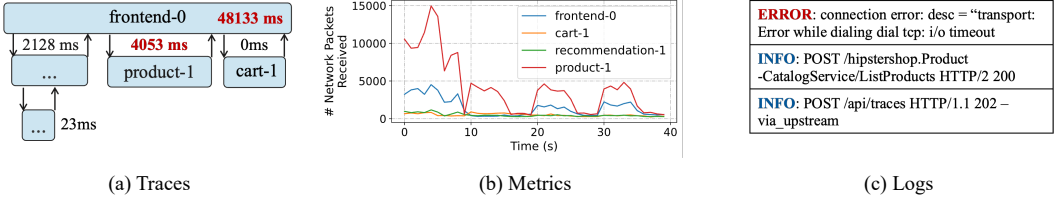


Fig. 5. A real case of multimodal monitoring data.

An operator might pinpoint the culprit instance *product-1* by analyzing captured traces. However, determining the failure type (Net-packets-loss) would be challenging due to insufficient details on network packets in traces. To further identify the failure type, the operator would need to check for keywords such as "tcp: i/o timeout" in the logs. If the logs lack relevant information, the operator would have to observe and analyze various metrics. Finally, the operator would confirm the failure type as Net-packets-loss due to a significant decrease in the number of network packets received by *product-1*. To sum up, it is plausible to integrate the superiority of three modal information for failure diagnosis.

### 3.2 Preferences and View-invariance in Multimodal Data

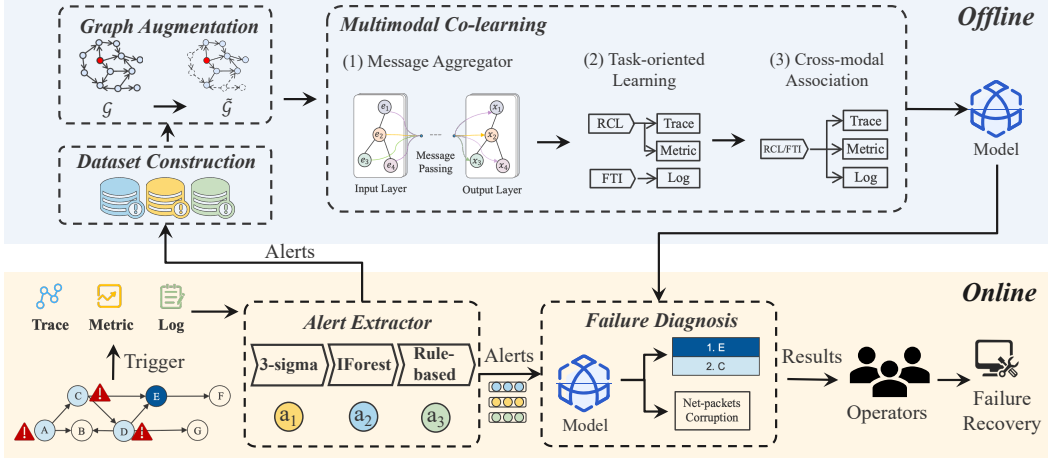
During our empirical diagnosis of failures using multimodal monitoring data, we observed intriguing phenomena and patterns that provide valuable insights for our design.

Firstly, we noticed a significant disparity in the contribution of each modality to different diagnosis tasks. Fig. 5 shows a motivating example concerning Net-packets-loss failure in a microservice-based system. As mentioned in Section 2, messages in ERROR-level logs often record information about failure types, indicating a preference for the log modality in the FTI task. In this example, the "tcp:i/o timeout" in the ERROR-level log suggests a network-related failure type. In addition, by analyzing the execution path and instance status displayed in the trace, we can deduce an abnormal invocation pair (i.e., *frontend-0*→*product-1*), which indicates that the root cause lies in the downstream instance *product-1*. Metrics show a significant downward trend in the network packets received by *product-1*. Coupled with the "tcp:i/o timeout" provided by the logs, we can infer that the failure type is Net-packets-loss rather than reduced workload. This indicates that metrics and traces are crucial for the RCL task, while logs and metrics are important for identifying failure types. These observations suggest that different tasks exhibit biases towards certain modalities, necessitating unequal attention to each modality in specific diagnostic tasks.

Secondly, multimodal monitoring data share some view-invariant information when a failure occurs. Although each modality offers distinct perspectives on system status, certain shared information is shared across multiple modalities. We refer to this shared information as view-invariant information. As shown in Fig. 5, we can independently infer the system status (i.e., "abnormal") through abnormal latency in traces, irregular metric fluctuations, or ERROR-level logs. We can also deduce the abnormal phenomenon (i.e., "performance degradation") based on the high latency of traces or "timeout" keywords in logs. Besides, normal instances (e.g., "cart-1") are identifiable in traces and metrics. The exploration and amplification of this view-invariant information facilitate the construction of cross-modal associations, contributing to the reduction of the scope of failure diagnosis.

## 4 APPROACH

Fig. 6 depicts the overall structure of our proposed multimodal failure diagnosis framework, *TVDiag*, encompassing an offline training phase and an online diagnosis phase. During the offline training

Fig. 6. Overview of *TVDiag*.

phase, we separately extract alerts from historical multimodal monitoring data and subsequently transform them into an alert dataset. *TVDiag* then trains a diagnosis model based on this pre-constructed multimodal dataset. In the online diagnosis phase, alerts are extracted in real time from multimodal data, and the diagnosis model is utilized to predict root causes and failure types.

The offline training process is composed of three components: (1) Dataset construction: *TVDiag* collects alerts from an online alert extractor, creating a unified alert dataset prepared for training (§ 4.1). (2) Graph augmentation: To enrich the training alert dataset and enhance the generalizability of the diagnosis model, we design a graph-based data augmentation strategy by randomly inactivating non-root cause microservice instances (§ 4.2). (3) Multimodal co-learning: Considering the preference of diagnosis tasks for specific modalities, we propose a task-oriented learning method to amplify modality-specific advantages. Furthermore, we establish cross-modal associations using contrastive learning to extract view-invariant failure information (§ 4.3).

In the online diagnosis phase, *TVDiag* first extracts alerts from multimodal monitoring data and diagnoses failures for alerts based on the trained model. The whole procedure comprises two components: (1) Alert extractor: This component uniformly extracts alerts from logs, traces, and metrics based on heuristic rules. Next, *TVDiag* transforms these alerts into learnable features, which are then utilized for online diagnosis and stored as historical failure patterns for offline training (§ 4.1). (2) Failure diagnosis: The objective of this component is to fuse multimodal alert features to localize root causes and determine failure types (§ 4.4).

#### 4.1 Dataset Construction

In this section, we collect alerts from the online system and construct an alert dataset for training. As shown in Fig. 6, the data source for dataset construction is the online alert extractor module. To help readers better understand the composition of the alert dataset, we include an introduction to the preliminary module, the alert extractor.

**Alert Extractor:** This module abstracts valuable information from multimodal data and transforms it into learnable features that can be optimized for downstream diagnosis tasks. The variation in the collection interval and the heterogeneity in data structure pose challenges to the alignment of multimodal data. Inspired by DiagFusion [68], *TVDiag* separately converts multimodal, heterogeneous monitoring data into unified alerts. These alerts document anomalies from multimodal data using fixed text templates, facilitating straightforward encoding into learnable semantic features.

Table 1. Templates and examples of extracted alerts.

Modality	Alert Template	Example
Metric	$(reporterId, metricName)$	( <i>product-1</i> , "networkReceiveMB")
Trace	$(reporterId, parentId, abnormalType)$	( <i>product-1</i> , "frontend-0", "500")
Log	$(reporterId, logKey)$	( <i>product-1</i> , "13")

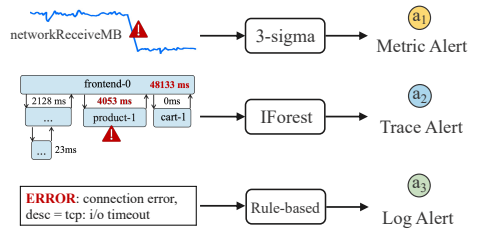


Fig. 7. Illustration of alert extractor.

More specifically, *TVDiag* detects alerts from metrics, logs, and traces across all microservice instances. Table 1 presents the templates and examples of alerts for each modality. The common element shared among all templates is defined as  $(reporterId, *)$ , where *reporterId* represents the unique ID of the microservice instance reporting the alert, and  $*$  records the modality-specific information. Fig. 7 depicts an overview of the alert extractor.

(1) **Trace Alert.** We adopt the Isolation Forest (IForest) [36] to detect anomalies and generate alerts based on the response time and status code of each invocation pair from traces. As a widely used anomaly detection method, IForest constructs decision trees by randomly isolating data points and identifies anomalies by observing the average path length required to isolate them. The extraction performance of IForest will be further discussed in section 5.3. Operators typically detect system failures through interactions, response times, and status codes in traces [15]. High response time often implies performance degradation, while abnormal status codes indicate business errors. Here,  $*$  is elaborated as  $(parentId, abnormalType)$ , capturing the caller of the reporter instance and the current abnormal type. Note that we define the abnormal type here as either abnormal status codes or performance degradation (PD). For example, the alert ("*product-1*", "frontend-0", "500") indicates that the status code for the invocation pair (*frontend-0*  $\rightarrow$  *product-1*) is abnormal. Meanwhile, the alert ("*product-1*", "frontend-0", "PD") signifies that the invocation pair has a notably high latency.

(2) **Metric Alert.** Due to the potential generation of thousands of metrics in a microservice system, training a separate IForest model for each metric incurs significant time overhead. Consequently, we opt for the 3-sigma rule [46], which, while slightly less performant, offers rapid processing speed as an alternative. For a given metric (e.g., *networkReceiveMB*) under inspection, we collect the numerical fluctuations  $[m_1, m_2, \dots, m_n]$  over a time period. Subsequently, we compute the mean  $\mu$  and standard variance  $\sigma$  for these fluctuations. If  $|m_n - \mu|$  exceeds  $3\sigma$ , it is deemed indicative of an alert in this metric, and the metric name is recorded as an alert.

(3) **Log Alert.** As depicted in [8, 9, 18], a semi-structured log message can be parsed into a fixed part (i.e., *logKey*) and a variable part. For example, the *logKey* for the log "upload business logs on 2021-08-15 failed" is "upload business logs on # failed." *TVDiag* parses logs using Drain [18] and matches each log with a *logKey*. In terms of log alert production, DiagFusion [68] randomly samples a batch of *logKeys* as alerts. However, several high-frequency *logkeys* occupy the majority of total logs [63]. Besides, these high-frequency *logkeys* contain numerous redundant information that is useless for failure diagnosis, such as records of common queries. Random sampling risks preserving this redundancy and overlooking low-frequency *logKeys*, especially those with **ERROR** levels, which are generally rare and valuable in the collected logs. To alleviate this problem, *TVDiag* employs two rules for alert generation:

- **Rule 1:** All **ERROR**-level *logKeys* are treated as alerts.

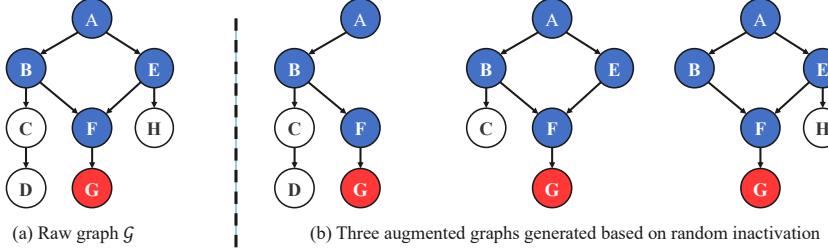


Fig. 8. Example of graph augmentation. The red node is the root cause of the current failure, the blue nodes are abnormal instances, and the blank nodes denote normal instances. All augmented individuals are essentially subgraphs derived from the raw graph.

- **Rule 2:** The top- $k$   $\log\text{Keys}$  with the lowest occurrence frequency in history are treated as alerts. Using these two rules,  $TV\text{Diag}$  retains low-frequency abnormal  $\log\text{Keys}$  as alerts while eliminating the redundancy of high-frequency  $\log\text{Keys}$ .

**Alert Embedding and Dataset Preparation:** For each historical failure, we extract alerts from three modalities and build a correlation graph  $\mathcal{G} = \langle \mathcal{V}, \mathcal{E} \rangle$ , where  $\mathcal{V}$  is a set of microservice instances, and  $\mathcal{E}$  is a set of invocation pairs from traces. Each alert is assigned to the corresponding microservice instance  $v_i$  ( $v_i \in \mathcal{V}$ ) based on the *reporterId*. For the  $i$ -th microservice instance  $v_i$ , DiagFusion regards alerts of three modalities as a sentence, with each alert considered a word, and utilizes fastText [4], a word embedding technology widely used in natural language processing, to encode the alerts into a learnable feature. However, prematurely merging the alerts of three modalities into one feature is not conducive to extracting the high-dimensional information unique to each modality. In contrast, for each instance  $v_i$ ,  $TV\text{Diag}$  transforms alerts of different modalities into a tuple of features, denoted as  $\mathbf{H}_i = (\mathbf{H}_i^M, \mathbf{H}_i^T, \mathbf{H}_i^L)$ , where  $\mathbf{H}_i^M$ ,  $\mathbf{H}_i^T$ , and  $\mathbf{H}_i^L$  denote the features of metrics, traces, and logs in microservice instance  $v_i$ , respectively. We combine the correlation graph  $\mathcal{G}$  and the corresponding alert features of all historical failures into the alert dataset.

## 4.2 Graph Augmentation

Manually scrutinizing a large volume of monitoring data and subsequently labeling failures is extremely arduous. To mitigate the problem of inadequate labeled data and enhance the generalizability of our framework, we implement a graph-based data augmentation strategy that involves random inactivation for non-root cause microservice instances. The underlying rationale of this strategy is that the lack of observability for some non-root cause microservice instances has little impact on the judgment of the root cause and failure type. We classify non-root cause microservice instances into abnormal and normal ones. Disabling the observability in normal microservice instances will not significantly affect failure diagnosis, as confirmed by existing anomaly-based failure diagnosis methods [32, 58, 70]. Meanwhile, the absence of observability in some abnormal non-root cause microservice instances does simulate pod-killing scenarios, enhancing  $TV\text{Diag}$  to adapt to situations with incomplete observability.

Based on the above motivations, we can reasonably hypothesize that inactivating a small proportion of non-root cause nodes will not significantly alter the semantic information of the graph  $\mathcal{G}$ . Inspired by the node-dropping strategy proposed by GraphCL [61], we design a graph-based data augmentation method. As depicted in Fig. 8, for the instance correlation graph  $\mathcal{G}$ ,  $TV\text{Diag}$  randomly discards  $m$  nodes along with their related edges to generate an augmented graph  $\tilde{\mathcal{G}}$ . Here we calculate  $m$  as:

$$m = \lfloor p \cdot |\mathcal{V}| \rfloor, \quad (2)$$

where  $p$  denotes the inactivation probability and  $|\mathcal{V}|$  is the number of microservice instances. We apply the graph augmentation strategy to each sample in the training alert dataset, generating a mutated instance correlation graph  $\tilde{\mathcal{G}}$  corresponding to the original graph  $\mathcal{G}$ . Notably,  $\tilde{\mathcal{G}}$  and  $\mathcal{G}$  share the same root cause and failure type. By incorporating  $\tilde{\mathcal{G}}$  into the training dataset, we alleviate data scarcity issues and enhance the model performance.

### 4.3 Multimodal Co-learning

*TVDiag* shares and integrates knowledge among different modalities by co-learning multimodal features. Considering the failure propagation between microservices [58, 62], *TVDiag* performs message passing and feature aggregation to obtain graph-level features for each modality. In this process, we conduct task-oriented learning to enhance the advantages of specific modalities under corresponding tasks. Moreover, *TVDiag* builds cross-modal associations based on contrastive learning for three modalities, enabling the proposed method to extract the invariant information for failures from different views.

**Message Aggregator:** Given the instance correlation graph  $\mathcal{G}$  (or the augmented graph  $\tilde{\mathcal{G}}$ ) in the training dataset, *TVDiag* performs message passing with three graph encoders on the features of each modality to simulate failure backtracking. Three alert features  $(\mathbf{H}_k^M, \mathbf{H}_k^T, \mathbf{H}_k^L)$  serve as the initial embeddings of each node  $v_k$  in  $\mathcal{G}$ . By distilling high-dimensional representation of neighborhoods, all nodes assimilate alert information from others and update their own embeddings. Herein, we leverage GraphSAGE [16] as the backbone of each layer in graph encoders. Unlike training distinct embeddings for each node, GraphSAGE emphasizes learning the aggregation process from neighborhoods, which better aligns with the extraction of failure backtracking patterns in our scenario. Generally, we set up multi-layer GraphSAGEs to enable nodes to perceive the topology and node feature information of a larger neighborhood. Let  $\mathbf{E}_k^l$  denote the  $l$ -th layer embedding of node  $v_k$ . Note that  $\mathbf{E}_k$  can be replaced by any one of  $\mathbf{H}_k^M$ ,  $\mathbf{H}_k^T$ , or  $\mathbf{H}_k^L$ . We update node embeddings according to:

$$\mathbf{E}_{I(k)}^{l+1} = \text{aggregate} \left( \{\mathbf{E}_j^l, \forall j \in I(k)\} \right), \quad (3)$$

$$\mathbf{E}_k^{l+1} = \sigma \left( \mathbf{W} \cdot \text{concat}(\mathbf{E}_k^l, \mathbf{E}_{I(k)}^{l+1}) \right), \quad (4)$$

$$\mathbf{E}_k^{l+1} = \mathbf{E}_k^{l+1} / \|\mathbf{E}_k^{l+1}\|_2, \quad (5)$$

where  $I(k)$  is the immediate neighborhood of  $v_k$ .  $\mathbf{E}_k^{l+1}$  represents the new node embedding of  $v_k$  that concats the information of neighborhoods  $(\mathbf{E}_{I(k)}^{l+1})$ .  $\text{aggregate}$  and  $\mathbf{W}$  denote the learnable aggregator function and weight matrix.  $\sigma$  represents the nonlinear activation function. After traversing three GraphSAGE layers, we can obtain the graph-level feature by summarizing all node embeddings  $\mathbf{E}_k$  in  $\mathcal{G}$  through a maxPooling layer. More concretely, the graph-level feature  $\mathbf{F}$  can be calculated as:

$$\mathbf{F} = \max_{1 \leq k \leq |\mathcal{V}|} (\mathbf{E}_k). \quad (6)$$

In other words,  $\mathbf{F}$  is the maximum value of all node embeddings in  $\mathcal{G}$ . We apply the above operations to the node embeddings of each modality, yielding three graph-level features, i.e.,  $\mathbf{F}^M$ ,  $\mathbf{F}^T$ , and  $\mathbf{F}^L$ .

**Task-oriented Learning:** Rather than directly fusing the graph-level features of three modalities, *TVDiag* amplifies the potential contribution of each modality to corresponding tasks. The fundamental principle is to maximize the agreement among modality-specific features that share the same task label. To illustrate the process of task-oriented learning, we take the root cause localization (RCL) task with the trace modality as an example, noting that this approach can be applied to other modalities and tasks as well. For the RCL task, we posit that two sets of traces

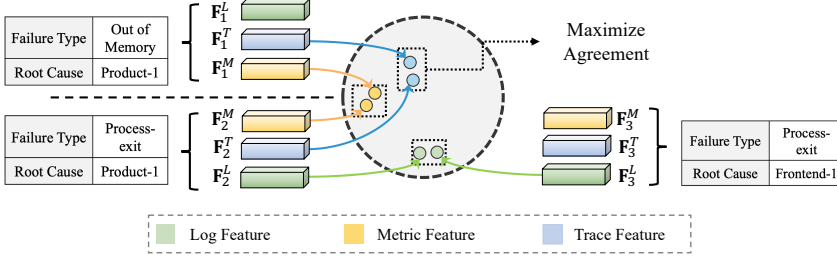


Fig. 9. Examples of task-oriented learning.

with the same root cause should exhibit maximum coherence at the feature level. This is because the affected microservices and the failure paths caused by the same culprit are likely to be similar. Let  $S = \{s_1, s_2, \dots, s_n\}$  represent a mini-batch with  $n$  failure samples in the training dataset, where each sample  $s_i = (\mathbf{F}_i^T, y_i)$  contains a graph-level trace feature  $\mathbf{F}_i^T$  and a root cause  $y_i$ . As shown in Fig. 9, we strive to bring the trace features ( $\mathbf{F}_1^T$  and  $\mathbf{F}_2^T$ ) of two samples with the same root cause ( $E$ ) closer in the feature space, extracting their shared knowledge about the root cause.

We adopt a supervised contrastive learning approach [5, 22] to enhance the agreement between trace features sharing the same root cause. We define the positive set of  $s_i$  as  $P(i) = \{j|j \in [1, n], j \neq i, y_j = y_i\}$ , and the negative set as  $N(i) = \{j|j \in [1, n], y_j \neq y_i\}$ . Hence, we formulate the task-oriented loss for trace  $\mathcal{L}_{to}^T$  as:

$$\mathcal{L}_{to}^T = \sum_{i=1}^n \frac{-1}{|P(i)|} \sum_{j \in P(i)} \ln \left[ \frac{\phi(\mathbf{F}_i^T, \mathbf{F}_j^T)}{\phi(\mathbf{F}_i^T, \mathbf{F}_j^T) + \sum_{z \in N(i)} \phi(\mathbf{F}_i^T, \mathbf{F}_z^T)} \right], \quad (7)$$

where  $\phi(\mathbf{F}, \mathbf{F}')$  measures the distance between two features  $F$  and  $\mathbf{F}'$ .  $\phi(\mathbf{F}, \mathbf{F}')$  is calculated by:

$$\phi(\mathbf{F}, \mathbf{F}') = \exp(\text{sim}(\mathbf{F}, \mathbf{F}') / \tau), \quad (8)$$

where  $\tau$  is the temperature parameter that adjusts the attention to difficult samples [53].  $\text{sim}(\cdot)$  measures the similarity (e.g., the cosine similarity) between two features. In this way, *TVDiag* can effectively identify the common and effective information of one modality by magnifying the similarity between the specific-modality samples under the same root cause.

We employ RCL as guidance for the feature learning process of traces and metrics. Additionally, the abundant failure details present in logs play a crucial role in the FTI task [66]. The task-oriented loss  $\mathcal{L}_{to}$  for the three modalities can be expressed as:

$$\mathcal{L}_{to} = \mathcal{L}_{to}^T + \mathcal{L}_{to}^M + \mathcal{L}_{to}^L, \quad (9)$$

where  $\mathcal{L}_{to}^M$  and  $\mathcal{L}_{to}^L$  denote the task-oriented loss for metrics and logs, respectively.

**Cross-modal Association:** Different modalities provide varying views of the same failure. These modalities share some hidden view-invariant information, such as abnormal microservice instances, abnormal periods, and failure degrees. Motivated by this, we preserve the view-invariant information by building cross-modal associations through contrastive learning.

Given a mini-batch of samples  $S = \{s_1, s_2, \dots, s_n\}$ , where each sample  $s_i = (\mathbf{F}_i^M, \mathbf{F}_i^T, \mathbf{F}_i^L)$  contains the features of three modalities for a failure, we set metrics as the core view and seek to bring other views (i.e., traces and logs) closer to metrics for each sample  $s_i$ . Metrics are suitable as the core view of cross-modal association because they share many commonalities with other modalities in various tasks. As mentioned in Section § 3.2, both metric types and log messages are usually utilized to assess the system status and failure phenomena. Besides, there is common information

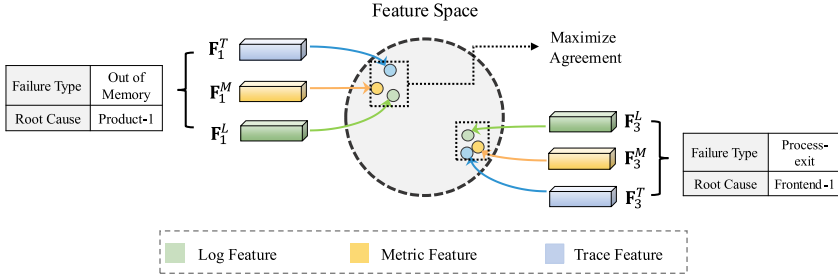


Fig. 10. Examples of cross-modal association.

between metrics and traces in identifying normal microservices. As shown in Fig. 10, *TVDiag* treats  $(\mathbf{F}_i^M, \mathbf{F}_i^T, \mathbf{F}_i^L)$  as positive tuples that should be tightly clustered in the feature space, while features of other samples with different root causes or failure types are dispersed. We minimize the distances between  $\mathbf{F}_i^M$  and  $\mathbf{F}_i^T$ ,  $\mathbf{F}_i^M$  and  $\mathbf{F}_i^L$  separately, achieving closer proximity among the three modalities. The learning objective of closing two modalities  $D_1$  and  $D_2$  is defined as:

$$\mathcal{L}_{cm}^{D_1 \sim D_2} = \frac{1}{2n} \sum_{i=1}^n \left( l\left(\mathbf{F}_i^{D_1}, \mathbf{F}_i^{D_2}\right) + l\left(\mathbf{F}_i^{D_2}, \mathbf{F}_i^{D_1}\right) \right), \quad (10)$$

where  $l\left(\mathbf{F}_i^{D_1}, \mathbf{F}_i^{D_2}\right)$  represents the loss between two positives, and the loss is defined as follows:

$$l\left(\mathbf{F}_i^{D_1}, \mathbf{F}_i^{D_2}\right) = -\ln \frac{\phi\left(\mathbf{F}_i^{D_1}, \mathbf{F}_i^{D_2}\right)}{\sum_{a=1}^n \mathbb{1}_{a \neq i} \phi\left(\mathbf{F}_i^{D_1}, \mathbf{F}_a^{D_1}\right) + \sum_{b=1}^n \phi\left(\mathbf{F}_i^{D_1}, \mathbf{F}_b^{D_2}\right)}, \quad (11)$$

where  $\mathbb{1}_{a \neq i}$  takes on the value 1 if  $a \neq i$ , and 0 otherwise. The term  $\mathcal{L}_{cm}^{D_1 \sim D_2}$  is intended to facilitate the features of  $D_1$  and  $D_2$  in learning a more common consensus between them. We formulate the loss of cross-modal association as:

$$\mathcal{L}_{cm} = \mathcal{L}_{cm}^{M \sim T} + \mathcal{L}_{cm}^{M \sim L}, \quad (12)$$

where  $\mathcal{L}_{cm}^{M \sim T}$  represents the contrastive loss between metric features and trace features, and  $\mathcal{L}_{cm}^{M \sim L}$  signifies the contrastive loss between the metric features and log features. Guided by the loss of cross-modal association  $\mathcal{L}_{cm}$ , the view-invariant information between different modalities is effectively amplified.

#### 4.4 Failure Diagnosis

To comprehensively consider the information from all three modalities and perform failure diagnosis without loss of information, *TVDiag* concatenates the features  $\mathbf{F}^M$ ,  $\mathbf{F}^T$ , and  $\mathbf{F}^L$  to obtain the final fused feature:

$$\mathbf{F} = \mathbf{F}^M \oplus \mathbf{F}^T \oplus \mathbf{F}^L. \quad (13)$$

The fused feature  $\mathbf{F}$  serves as the input for downstream failure diagnosis tasks. Intuitively, root cause localization (RCL) and failure classification (FTI) can benefit from shared knowledge, such as the category of abnormal metrics, unusual log templates, and abnormal microservices, among others. Therefore, RCL and FTI can be regarded as two complementary multi-classification tasks that share knowledge. Accordingly, we train these two diagnosis tasks jointly, leveraging the shared knowledge to enhance the learning of each other. To achieve this, we leverage two multilayer

perceptrons (MLPs) to solve them jointly, increasing the performance of both subtasks while saving training and inference time.

For the RCL task, we choose the cross-entropy loss to quantify the discrepancy between predicted root causes and actual ones:

$$\mathcal{L}_{rcl} = -\frac{1}{T} \sum_{i=1}^T \sum_{j=1}^N y_{i,j} \log(p_{i,j}), \quad (14)$$

where  $T$  denotes the number of samples and  $N$  is the total number of microservice instances. Here,  $y_{i,j} = 1$  if the root cause of the  $i$ -th sample ( $s_i$ ) is  $j$ , and 0 otherwise. The value  $p_{i,j}$  represents the probability of determining the root cause of  $s_i$  as  $j$ . Similarly, for the FTI task,  $TVDiag$  defines the loss as:

$$\mathcal{L}_{fti} = -\frac{1}{T} \sum_{i=1}^T \sum_{k=1}^C y_{i,k} \log(p_{i,k}), \quad (15)$$

where  $C$  indicates the number of failure types.  $y_{i,k} = 1$  if the failure type of the  $i$ -th sample is  $k$ , and 0 otherwise. Because  $\mathcal{L}_{to}$  and  $\mathcal{L}_{cm}$  are essentially contrastive losses, we add them directly and scale the sum by multiplying a hyper-parameter  $\delta$  to get  $\mathcal{L}_{con}$ , i.e.,  $\mathcal{L}_{con} = \delta \cdot (\mathcal{L}_{to} + \mathcal{L}_{cm})$ . The overall loss is a combination of three components:

$$\mathcal{L} = \alpha \cdot \mathcal{L}_{con} + \beta \cdot \mathcal{L}_{rcl} + \gamma \cdot \mathcal{L}_{fti}, \quad (16)$$

where  $\alpha$ ,  $\beta$ , and  $\gamma$  are weighting factors for each component. To avoid assigning static weights that might be suboptimal, we follow the method [31] and convert the static weights ( $\alpha$ ,  $\beta$ , and  $\gamma$ ) into learnable parameters that can be dynamically tuned during model training. Equation 16 is then reformulated as:

$$\mathcal{L} = \sum_{1 \leq z \leq 3} \frac{1}{2 \cdot \theta_z^2} \cdot \mathcal{L}(z) + \ln(1 + \theta_t^2), \quad (17)$$

where  $\theta_z$  is the learnable parameters and  $\mathcal{L}(z)$  represents the loss of each component, i.e.,  $\mathcal{L}_{con}$ ,  $\mathcal{L}_{rcl}$  or  $\mathcal{L}_{fti}$ .

Finally,  $TVDiag$  generates a ranking list  $\mathcal{R}$  for RCL and identifies a failure type  $t$  for FTI. These results narrow down the diagnosis scope and guide operators in making recovery decisions.

## 5 EVALUATION

To examine the effectiveness of the proposed  $TVDiag$ , we conducted comparisons with state-of-the-art failure diagnosis methods on two datasets. This section will answer the following research questions:

### – RQ1: How does $TVDiag$ perform compared to existing methods?

The failure diagnosis encompasses two tasks: root cause localization (RCL) and failure type identification (FTI). For the RCL task, we assessed and compared our method with four single-modal baselines and two multimodal methods. For the FTI task, we compared  $TVDiag$  with a log-based method and a multimodal approach. Additionally, we derived three traditional machine learning methods from  $TVDiag$  as supplementary baselines.

### – RQ2: What is the effectiveness of each component in $TVDiag$ ?

$TVDiag$  consists of five main modules: alert extractor, graph augmentation (AUG), task-oriented learning (TO), cross-modal association (CM), and dynamic weights (DW). To investigate the contribution of these modules, we conducted an ablation study by individually removing each one.

### – RQ3: How do hyper-parameters influence $TVDiag$ ?

Table 2. Dataset Statistics

Dataset	# Microservices	# Instances	# Failure Types	# Records		# Types	
$\mathcal{A}$	5	10	5	Metric	217,461,390	Metric	6640
				Trace	3,084,066	Trace	122
				Log	87,974,577	Log	49
$\mathcal{B}$	10	40	9	Metric	25,914,595	Metric	404
				Trace	63,283,650	Trace	63
				Log	58,345,509	Log	23

*TVDiag* includes several hyper-parameters, such as the inactivation probability  $p$ , the contrastive loss scale  $\delta$ , the number of graph layers  $l$ , and the temperature parameter  $\tau$ . We conducted comprehensive comparison experiments on each hyper-parameter to verify their effect.

– **RQ4: How does each modality impact the two diagnosis tasks in *TVDiag*?**

Integrating multimodal monitoring data is crucial for failure diagnosis. We performed comparison experiments by ablating one or two modalities to investigate their contribution to failure diagnosis. To ascertain the mutual effect between two fundamental failure diagnosis tasks, we calculated their inter-task affinity during the training process.

## 5.1 Experimental Design

**Datasets:** Experiments were conducted on two open-source microservice datasets ( $\mathcal{A}$  and  $\mathcal{B}$ ) with multimodal monitoring data, where  $\mathcal{A}$  is derived from the GAIA dataset<sup>3</sup>, and  $\mathcal{B}$  is based on the AIOps-22 dataset<sup>4</sup>. Table 2 shows the statistics of both datasets.

- **Dataset  $\mathcal{A}$ .** The GAIA dataset has been widely employed as an evaluation dataset in various papers [51, 68, 69]. It records metrics, traces, and logs from the MicroSS simulation system in July 2021. MicroSS is a business simulation system that consists of ten microservices and several middleware components like Redis, MySQL, and Zookeeper. To simulate real-world failures, various types of instance-level failures, such as memory anomalies and login failures, were intentionally injected into MicroSS.
- **Dataset  $\mathcal{B}$ .** The AIOps-22 dataset originates from the training data released by the AIOps 2022 Challenge, where failures across three levels (node, service, and instance) were injected into a Web-based e-commerce platform. To replicate a scenario involving a microservice-based online system with large-scale multimodal monitoring data, AIOps-22 collected four business metrics, 400 performance metrics, traces, and logs to describe the status of running microservices. To align with the failure level of the GAIA dataset, we retained 113 instance-level failure records, which were manually injected by the sponsor.

**Competing Approaches:** We utilized state-of-the-art multimodal and single-modal methods in RCL and FTI, respectively, as baselines. For the RCL task, we considered the following methods:

- **DiagFusion** [68] is a multimodal method that fuses all modalities during data preparation by consolidating them into events. Subsequently, these events are encoded with two topology-adaptive graphs for downstream diagnosis tasks. For RCL and FTI tasks, DiagFusion statically assigns equal weights to the two tasks and performs joint learning using two topology adaptive graph convolution networks.
- **Eadro** [23] presents a multimodal failure diagnosis framework that integrates anomaly detection and RCL. It designs separate feature extractors for three modalities and then fuses

<sup>3</sup><https://github.com/CloudWise-OpenSource/GAIA-DataSet>

<sup>4</sup><https://competition.aiops-challenge.com>

the multimodal features. Using the graph attention networks, Eadro learns the dependency-aware status of microservices and optimizes the fused feature in the downstream diagnosis task.

- **MicroRank** [62] is a trace-based diagnosis method for the RCL task, synthesizing the Pagerank algorithm and spectrum analysis to infer root causes.
- **TraceRCA** [28] proposes a trace-based root cause localization framework. It first mines several suspicious service sets using the FP-Growth algorithm. For each microservice within these sets, TraceRCA scores it according to the discrepancies between the number of abnormal and normal traces.
- **MicroRCA** [58] introduces a metric-based diagnosis method that utilizes the Pagerank algorithm to pinpoint the root cause within the anomalous subgraph.
- **NicroHECL** [35] is a metric-based root cause localization approach that dissects the golden metrics to analyze failure propagation and rank candidate microservices.

For the FTI task, we chose a log-based method and DiagFusion as the baseline. Besides, we derived three variants of *TVDiag* by replacing the multimodal co-learning module with three traditional machine-learning methods:

- **LogCluster** [33] is a log-based problem identification method that categorizes failures by clustering logs and matching them with a knowledge base.
- **DT-FTI** is a variant of *TVDiag* that sets the failure diagnosis model as a decision tree (DT). It concatenates the multimodal alert features in § 4.1 and uses them as the input to this model, which outputs the classification results of failure types.
- **SVM-FTI** is a variant of *TVDiag* that replaces the failure diagnosis model with the support vector machine (SVM).
- **LGB-FTI** is a variant of *TVDiag* that replaces the failure diagnosis model with the typical ensemble model, i.e., LightGBM (LGB).

**Evaluation Criteria:** For RCL, a ranking list  $\mathcal{R}$  comprising root cause candidates is produced. We employed widely used  $HR@k$  (hit ratio of top- $k$ ),  $Avg@k$  (average hit ratio of top- $k$ ) [30, 58, 62], and  $NDCG@k$  (normalized discounted cumulative gain of top- $k$ ) [23, 34] to measure the performance of RCL.  $HR@k$  is formulated as:

$$HR@k = \frac{1}{N} \sum_{i=1}^N r_i \in \mathcal{R}_i[1:k], \quad (18)$$

where  $N$  is the number of all failures,  $\mathcal{R}_i[1:k]$  denotes the top- $k$  results of the  $i$ -th ranking list  $\mathcal{R}_i$ , and  $r_i$  is the ground truth for the  $i$ -th failure. The average hit ratio for top- $k$  results is defined as:

$$Avg@k = \frac{1}{k} \sum_{i=1}^k HR@i. \quad (19)$$

In general, the instances with higher ranks should inherently receive higher weights. We introduced  $NDCG@k$  to further assess the relevance of the top- $k$  results with the root cause:

$$NDCG@k = \frac{1}{N} \sum_{i=1}^N \sum_{j=1}^k \frac{rel_j}{\log_2(j+1)}, \quad (20)$$

where  $rel_j$  is 1 if the  $j$ -th instance of  $\mathcal{R}_i[1:k]$  is root cause, and 0 otherwise. Higher rankings of root causes imply better  $NDCG@k$  scores.

For the FTI task, we used typical classification indicators to measure the performance of baselines:  $Precision = \frac{TP}{TP+FP}$ ,  $Recall = \frac{TP}{TP+FN}$ , and  $F1\text{-score} = 2 \cdot \frac{Precision \cdot Recall}{Precision + Recall}$ , where  $TP$  and  $FP$  denote the

number of true-positive results and the number of false-positive results, respectively.  $FN$  represents the number of samples whose failure types are not identified. Higher values of these metrics indicate better performance.

**Implementation Details:** For the division of the training and test sets in dataset  $\mathcal{A}$ , we followed the division method proposed by DiagFusion [68], which splits 160 training samples and 939 testing samples based on the sample collection time. For dataset  $\mathcal{B}$ , we used 80% of the data for training and the remaining 20% for testing. The alert embedding dimension was set to 128. We set the dimension of the hidden layer in GraphSAGE to 64 and the output dimension to 32. Herein, we designated the aggregator function of GraphSAGE as LSTM to achieve better performance [16].

During model training, we used the Adaptive Moment Estimation (Adam) optimizer with an initial learning rate of  $1 \times 10^{-3}$  and a weight decay of  $1 \times 10^{-4}$ . To prevent overfitting and improve efficiency, we implemented an early stopping strategy based on changes in loss, halting the training process when the loss has not decreased for an extended period. The temperature parameter  $\tau$  was set to 0.3. The implementation of *TVDiag* was based on PyTorch 1.10.0 and DGL 1.0.1. All experiments were conducted on a workstation with a 24-core 12th Gen Intel(R) Core(TM) i9-12900 CPU and 128 GB of RAM. We publicized our source code and experimental data in [52].

## 5.2 Performance Comparison (RQ1)

**Objectives:** We investigate the effectiveness of *TVDiag* in RCL and FTI tasks by comparing it with existing single-modal and multimodal approaches. We further explore the performance of multimodal methods in root cause localization across different failure types.

**Experimental design:** Regarding the RCL task, we conducted a comparison experiment with four single-modal methods (i.e., MicroRCA, MicroHECL, TraceRCA, and MicroRank) and two multimodal methods, namely Eadro and DiagFusion. We adopted four metrics as the measurements:  $HR@1$ ,  $HR@3$ ,  $Avg@3$ , and  $NDCG@3$ . We further utilized the T-test to determine whether *TVDiag*'s performance on various metrics is significantly greater than that of the baseline methods. For the FTI task, we selected a typical log-based method (LogCluster) and a multimodal method (DiagFusion) as the baselines. More specifically, we replaced the backbone of *TVDiag* with three traditional machine learning models (SVM, DT, and LightGBM), concatenating alert features from the three modalities as input.

**Results:** Tables 3 and 4 present the evaluation results of different methods on the two datasets. *TVDiag* outperforms two state-of-the-art multimodal-based methods in the RCL task and the FTI task. As shown in Table 3, *TVDiag* significantly surpasses all baseline methods for the RCL task, achieving at least 55.94% improvement in  $HR@1$  accuracy and a 15.09% improvement in  $Avg@3$  compared to other methods. Compared to most baseline methods, the improvement of *TVDiag* in all metrics is significant, with a P-value less than 0.05. Particularly for dataset  $\mathcal{B}$  with more than 40 instances., *TVDiag* achieves a high  $HR@1$  accuracy of 0.76, indicating its robust ability to locate the root cause of failures despite the increased number of microservice instances. In contrast, DiagFusion underperforms in dataset  $\mathcal{B}$  because it first locates the microservice and then infers the failure instance based on the anomaly degree, which may mistakenly select those abnormal and non-root cause instances. It is worth noting that multimodal methods are consistently more effective than single-modal ones with regard to the RCL task, indicating that integration of multi-perspective data contributes to the performance of root cause localization.

For multimodal diagnosis methods, we further provided an intuitive representation of the performance across different failure types. As shown in Fig. 11, *TVDiag* yields a better performance than DiagFusion and Eadro across two datasets. This superiority is more pronounced in  $HR@1$ ,

Table 3. Root cause localization comparison.

Dataset	Modality	Method	P-value	HR@1	↑ HR@1	HR@3	↑ HR@3	Avg@3	↑ Avg@3	NDCG@3	↑ NDCG@3
$\mathcal{A}$	Metric	MicroRCA	1.2e-4	0.181	248.066%	0.385	109.351%	0.287	155.052%	0.298	146.644%
	Metric	MicroHECL	2.2e-5	0.118	433.898%	0.233	245.923%	0.177	313.559%	0.184	299.457%
	Trace	TraceRCA	6.4e-5	0.192	228.125%	0.364	121.429%	0.291	151.546%	0.295	149.153%
	Trace	MicroRank	2.6e-4	0.192	228.125%	0.419	92.363%	0.308	137.662%	0.321	128.972%
	Multimodality	Eadro	6.4e-3	0.304	107.237%	0.592	36.149%	0.473	54.757%	0.476	54.412%
	Multimodality	DiagFusion	1.8e-1	0.404	55.941%	0.801	0.624%	0.636	15.094%	0.685	7.299%
$\mathcal{B}$	Metric	MicroRCA	5.2e-7	0.058	1212.069%	0.155	471.613%	0.107	675.701%	0.113	638.053%
	Metric	MicroHECL	4.6e-7	0.044	1629.545%	0.142	523.944%	0.094	782.979%	0.100	734.000%
	Trace	TraceRCA	8.4e-6	0.150	407.333%	0.204	334.314%	0.183	353.552%	0.183	355.738%
	Trace	MicroRank	8.6e-6	0.171	345.029%	0.227	290.308%	0.205	304.878%	0.205	306.829%
	Multimodality	Eadro	4.3e-4	0.226	236.726%	0.478	85.356%	0.367	126.158%	0.374	122.995%
	Multimodality	DiagFusion	4.5e-6	0.205	271.220%	0.273	224.542%	0.239	260.870%	0.252	230.952%
	Multimodality	<b><i>TVDiag</i></b>	-	<b>0.761</b>	-	<b>0.886</b>	-	<b>0.830</b>	-	<b>0.834</b>	-

↑ indicates the improvement rate of ***TVDiag*** compared to other methods.

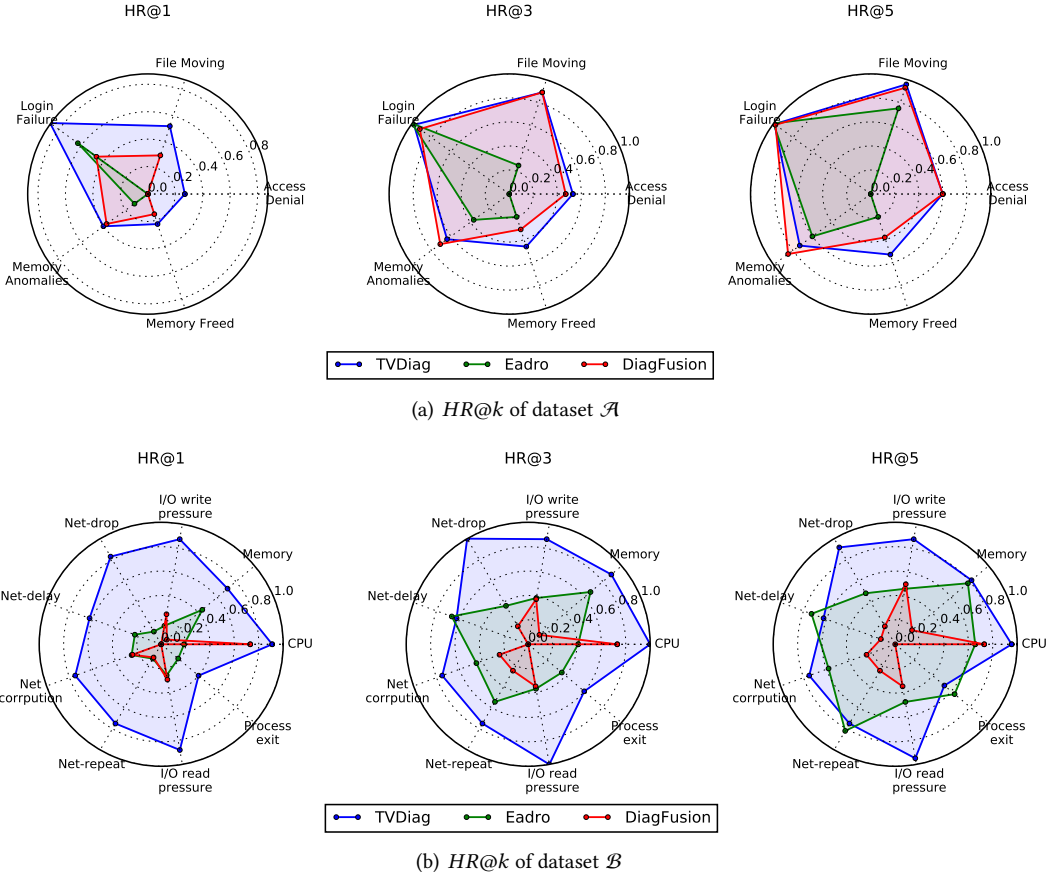
Table 4. Failure type identification comparison.

Dataset	Modality	Method	P-value	Precision	↑ Precision	Recall	↑ Recall	F1-score	↑ F1-score
$\mathcal{A}$	Log	LogCluster	6.4e-3	0.888	5.293%	0.915	4.481%	0.901	4.883%
	Multimodality	DiagFusion	1.5e-4	0.852	9.742%	0.838	14.081%	0.840	12.500%
	Multimodality	DT-FTI	5.3e-3	0.889	5.173%	0.892	7.175%	0.890	6.180%
	Multimodality	SVM-FTI	6.0e-2	0.883	5.889%	0.935	2.24%	0.908	4.075%
	Multimodality	LGB-FTI	2.6e-2	0.892	4.821%	0.928	3.017%	0.907	4.190%
	Multimodality	<b><i>TVDiag</i></b>	-	<b>0.935</b>	-	<b>0.956</b>	-	<b>0.945</b>	-
$\mathcal{B}$	Log	LogCluster	1.2e-2	0.434	96.774%	0.159	422.013%	0.147	465.306%
	Multimodality	DiagFusion	5.4e-5	0.533	60.225%	0.489	69.734%	0.505	64.554%
	Multimodality	DT-FTI	2.6e-6	0.448	90.625%	0.420	97.619%	0.422	96.919%
	Multimodality	SVM-FTI	8.9e-3	0.807	5.824%	0.784	5.867%	0.774	7.364%
	Multimodality	LGB-FTI	1.9e-4	0.604	41.391%	0.580	43.103%	0.556	49.460%
	Multimodality	<b><i>TVDiag</i></b>	-	<b>0.854</b>	-	<b>0.830</b>	-	<b>0.831</b>	-

manifesting as a larger coverage area. A higher *HR@1* indicates that operators incur fewer trial-and-error costs in root cause identification, enhancing diagnostic accuracy and failure recovery efficiency.

Table 4 depicts the performance comparison for the FTI task, which is measured by F1-score, *Precision*, and *Recall*. ***TVDiag*** can effectively identify the failure types, achieving the best F1-score, *Precision*, and *Recall* among all datasets. Compared to DiagFusion, which integrates all modalities in the alert extraction process, ***TVDiag*** demonstrates a substantial improvement in F1-score, achieving enhancements of more than 12.5% to 64.6% on two datasets. This underscores the efficacy of separately learning specific features for different modalities. LogCluster exhibits suboptimal performance in dataset  $\mathcal{B}$  due to the scarcity of informative log templates within this dataset. This phenomenon further illustrates the necessity of incorporating data from other perspectives (e.g., metrics) for the FTI task.

**Answer to RQ1:** For the RCL task, ***TVDiag*** significantly surpasses all baseline methods by 55.94% in *HR@1* and 15.09% in *Avg@3* across two datasets. In terms of the FTI task, ***TVDiag***

Fig. 11. Performance comparison of  $HR@k$  for different failure types.

demonstrates the most outstanding effectiveness, with an improvement rate of at least 4.08% compared to state-of-the-art baselines.

### 5.3 Ablation Study (RQ2)

**Objectives:** We aim to explore the contribution of different modules within *TVdiag*, including one module in the online diagnosis phase and four modules in the offline training phase.

**Experimental design:** As mentioned in Section 4, the training of *TVdiag* comprises four main components: graph augmentation (AUG), task-oriented learning (TO), cross-modal association (CM), and dynamic weights (DW). AUG denotes the graph augmentation that relies on random inactivation for non-root cause instances. TO and CM represent task-oriented learning and cross-modal association, respectively. DW dynamically assigns weights to each component in the overall loss  $\mathcal{L}$ . These derived methods can be summarized as follows:

- *TVdiag w/o AUG*: *TVdiag* ablates the graph augmentation module described in § 4.2.
- *TVdiag w/o TO*: *TVdiag* ablates the task-oriented learning module described in § 4.3.
- *TVdiag w/o CM*: *TVdiag* ablates the cross-modal association module described in § 4.3.

Table 5. Experimental results of the ablation study for graph augmentation (AUG), task-oriented learning (TO), cross-modal association (CM), and dynamic weights (DW). Note that the results for RCL are marked in blue, while the results for FTI are marked in gray.

Method	Dataset $\mathcal{A}$				Dataset $\mathcal{B}$			
	HR@1	HR@3	Avg@3	F1-score	HR@1	HR@3	Avg@3	F1-score
<i>TVDiag</i> w/o AUG	<b>0.633</b>	<b>0.809</b>	0.732	0.937	0.738	0.818	0.784	0.606
<i>TVDiag</i> w/o TO	0.619	0.795	0.723	0.934	0.682	0.807	0.761	0.734
<i>TVDiag</i> w/o CM	0.606	0.796	0.714	0.944	0.580	0.739	0.667	0.632
<i>TVDiag</i> w/o DW	0.619	0.783	0.714	0.945	0.534	0.636	0.583	0.596
<i>TVDiag</i>	0.630	0.806	<b>0.732</b>	<b>0.945</b>	<b>0.761</b>	<b>0.886</b>	<b>0.830</b>	<b>0.834</b>

Table 6. Performance comparison of alert extractors.

Dataset	Extractor	Method	Modality	HR@1	HR@3	Avg@3	F1-score
$\mathcal{A}$	IForest	<i>TVDiag</i>	Trace	<b>0.505</b>	<b>0.635</b>	<b>0.578</b>	<b>0.899</b>
	3-sigma	DiagFusion	Trace	0.398	0.604	0.504	0.731
	Rule-based	<i>TVDiag</i>	Log	<b>0.310</b>	<b>0.667</b>	<b>0.530</b>	<b>0.945</b>
	Sampling	DiagFusion	Log	0.301	0.644	0.508	0.877
$\mathcal{B}$	IForest	<i>TVDiag</i>	Trace	<b>0.511</b>	<b>0.773</b>	<b>0.667</b>	<b>0.653</b>
	3-sigma	DiagFusion	Trace	0.102	0.205	0.155	0.221
	Rule-based	<i>TVDiag</i>	Log	<b>0.432</b>	<b>0.693</b>	<b>0.639</b>	<b>0.578</b>
	Sampling	DiagFusion	Log	0.080	0.182	0.125	0.194

- *TVDiag* w/o DW: *TVDiag* statically assigning equal weights to all components of Equation 16.

In this section, we conducted a comprehensive ablation study across two datasets, comparing our proposed *TVDiag*, which includes all components, with the remaining four variants.

To further demonstrate that our enhanced alert extractor can capture more valuable information, we also conducted a performance comparison on all datasets by substituting it with the alert extractor of DiagFusion [68]. Since both methods share the same extraction strategy for metrics, no comparison is necessary in that aspect. We utilized these two alert extractors to separately generate alert datasets for both trace and log modalities. Subsequently, we conducted failure diagnosis on the two extracted alert datasets, eliminating interference from other modalities.

**Results:** The results of the ablation study are listed in Table 5. We elaborate four key results as follows: (1) Our task-oriented learning module makes a macroscopic contribution, as *TVDiag* achieves superior performance on both datasets when compared to *TVDiag* w/o TO. This is mainly because the TO component maximizes the agreement among samples of a specific modality that share the same task label, facilitating the extraction of useful potential information for that task. (2) Indispensable view-invariant information exists across different modalities. *TVDiag* outperforms *TVDiag* w/o CM on all measurements, especially in dataset  $\mathcal{B}$ , owing to the preservation of view-invariant information (e.g., system status and normal microservices). (3) The integration of graph augmentation reinforces the overall failure diagnosis. The graph augmentation (AUG) method involves a node-dropping strategy simulating the missing data phenomenon in data collection, enhancing the generalization of *TVDiag*, thereby increasing the F1-score by 18.81% on average. Note that the HR@1 and HR@3 are slightly poorer after integrating AUG on dataset  $\mathcal{A}$ . This is mainly

because dataset  $\mathcal{A}$  contains limited instances, losing important information after node inactivation, such as removing critical abnormal relay microservices. Moreover, TO and CM usually require sufficient data in a batch to support contrastive learning. The AUG here alleviates the problem of insufficient data and the expensive cost of manual labeling. (4) The DW module adaptively balances the training process of the RCL and FTI tasks, thereby promoting the overall effectiveness of *TVDiag*. The variant that ablates dynamic weights exhibits decline across almost all evaluation metrics, respectively (21.42% on average), in both datasets compared to *TVDiag*. Finally, using all components of *TVDiag* together achieves the best performance across most evaluation criteria. In summary, all components of *TVDiag* contribute to the final performance.

As mentioned in Section 4.1, *TVDiag* employs the IForest method and a rule-based approach to extract alerts from traces and logs, respectively. In contrast, DiagFusion achieves the same functionality using the 3-sigma and sampling methods. As summarized in Table 6, the performance of the alert extractor in *TVDiag* surpasses that of DiagFusion across two modalities and two diagnosis tasks. The IForest extractor exhibits superior performance in the trace modality due to the robustness of the IForest model, which is capable of handling noise in a small number of traces. Concerning logs, the sampling method of DiagFusion may overlook low-frequency abnormal logs with significant value, leading to the loss of crucial information. In contrast, *TVDiag*'s two rules ensure that low-frequency abnormal logs are retained as alerts, providing robust criteria for failure diagnosis.

**Answer to RQ2:** The combination of four components (i.e., AUG, TO, CM, and DW) contributes to the performance of *TVDiag*, resulting in the highest *Avg@3* for RCL and F1-score for FTI. Our proposed alert extractor, which incorporates the IForest method and a rule-based approach, exhibits a noticeable improvement across all metrics to the baseline method.

#### 5.4 Sensitivity Analysis of Hyper-parameters (RQ3)

**Objectives:** We investigate the effect of four main hyper-parameters of *TVDiag*: the inactivation probability ( $p$ ), the scale factor ( $\delta$ ), the number of graph layers ( $l$ ), and the temperature parameter ( $\tau$ ).

**Experimental design:** The inactivation probability  $p$  controls the number of dropped nodes in the instance correlation graph  $\mathcal{G}$  in *TVDiag*. To measure the effect of different inactivation probabilities on the diagnosis task, we selected values for  $p$  within the range of 0.1 to 0.9. Because the contrastive loss  $\mathcal{L}_{con}$  in Eq. 16 is typically larger than the loss of the two diagnosis tasks (i.e.,  $\mathcal{L}_{rel}$  and  $\mathcal{L}_{fti}$ ), it is necessary to scale down the  $\mathcal{L}_{con}$  to prevent the model from neglecting the optimization of the failure diagnosis. We varied the contrastive loss scale  $\delta$  in the range of 0 to 0.9 and evaluated its impact. Additionally, we regulated the number of graph layers  $l$  from 1 to 4 to strike a balance between model performance and training time. The temperature parameter  $\tau$  used in Eq. 8 adjusts the contrast intensity between samples, thereby affecting the attention to difficult samples. We conducted experiments on  $\tau$  in the range of 0.1 to 0.9 and evaluated its impact.

**Results:** Fig. 12 presents the effectiveness ( $HR@1$ ,  $HR@3$ ,  $Avg@3$ , and F1-score) of these hyper-parameters across a range of values. Since the number of graph layers  $l$  significantly impacts efficiency, we also include the training time as a measurement for it.

– **Inactivation probability:** The principle of graph augmentation is equivalent to adding a batch of samples, which share the root cause labels of the original samples. Therefore, we can randomly deactivate a proportion  $p$  of non-root cause (non-label) pods to get an augmented sample. As shown in Fig. 12 (a), *TVDiag* achieves outstanding performance on both *Avg@3* and F1-score across two datasets when  $p=0.2$ . When the  $p$  is relatively small, the augmented graph

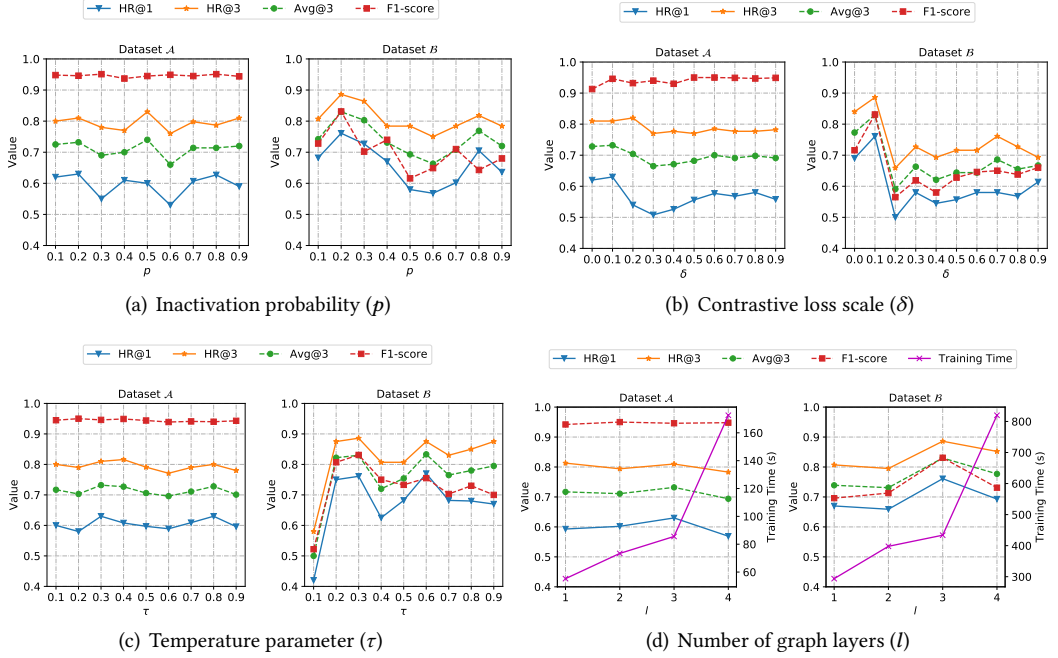


Fig. 12. Effect of the inactivation probability ( $p$ ), the contrastive loss scale ( $\delta$ ), the number of graph layers ( $l$ ), and the temperature parameter ( $\tau$ ).

differs slightly from the original graph, resulting in modest performance across two datasets. As the number of abandoned nodes increases, the remaining nodes receive information from only a limited number of neighborhoods, leading to the final graph-level feature focusing solely on the local information.

- **Contrastive loss scale:** The training objective of *TVDiag* is to optimize the performance of two diagnosis tasks and reduce the contrastive loss, which is the sum of losses from task-oriented learning and cross-modal association, namely  $\mathcal{L}_{con}$ . We adopt contrastive loss scale  $\delta$  to adjust the weight of  $\mathcal{L}_{con}$ . When  $\mathcal{L}_{con}$  is set to 0, it is equivalent to removing the TO and CM modules from *TVDiag*. Fig. 12 (b) depicts the performance of *TVDiag* for five scale factor settings on the two diagnosis tasks. When  $\delta = 0.1$ , *TVDiag* achieves the best performance in RCL and FTI tasks, indicating that the low  $\mathcal{L}_{con}$  indeed serves as a small portion of prior knowledge to guide *TVDiag* in learning view-invariant information and task-oriented features, rather than dominating the entire network’s training.
- **Temperature parameter:** When calculating the distance between two samples,  $\tau$  is used to smooth the similarity between two samples. A low  $\tau$  encourages the model to spotlight the disparity between the most similar and the most dissimilar sample pairs. Conversely, a high  $\tau$  indicates that the model is not sensitive to the difficult negative samples. Fig. 12 (c) illustrates the performance of failure diagnosis across various values of the temperature parameter  $\tau$ . *TVDiag* yields the best performance when  $\tau$  is set to 0.2.
- **Number of graph layers:** The number of graph layers  $l$  represents the depth of the model in propagating and aggregating information from neighborhoods. In theory, as  $l$  increases, the graph neural network can assimilate higher-order neighborhood information from more

distant nodes. However, deeper layers mean increased computational complexity and exacerbation of overfitting. As depicted in Fig. 12, *TVDiag* achieves the best performance while requiring modest training time when  $l$  is 3 across two datasets. Although there is a marginal increase in training time on both datasets when the  $l$  is set to 3. However, *TVDiag* outperforms the variant with  $l=2$  on dataset  $\mathcal{B}$  considerably, especially in  $HR@1$  and F1-score, showing an improvement of nearly 10%. Therefore, we set  $l$  as 3 on two datasets, which comes at the cost of slightly higher training time.

**Answer to RQ3:** *TVDiag* performs best with a suitable inactivation probability of 0.2 in augmented graphs. Regarding the training process, it can be observed that low-temperature parameters and low contrastive loss scales could have a positive effect on the final diagnosis performance. We set the number of graph layers as three in *TVDiag*, balancing the failure diagnosis performance and training consumption.

## 5.5 Impact Analysis of Modalities and Inter-Task Affinity (RQ4)

**Objectives:** We investigate the contribution of each modality, verifying the necessity of integration of multimodal data in failure diagnosis. Furthermore, we analyze the relationship between the RCL and FTI tasks by measuring their inter-task affinity.

**Experimental design:** To verify the hypothesis that the diagnosis tasks may be biased towards different modalities, we conducted experiments by discarding one or two modalities in *TVDiag*. For example, *w/o Metric* denotes a variant where the metric modality is discarded, while *w/ Metric* represents a variant where only the metric modality is retained. The omission of a modality is achieved by resetting all alert features of that modality to zero. Furthermore, we assessed the impact of different modalities in *TVDiag* by omitting one modality at a time.

Joint learning of two diagnosis tasks holds the promise of improving overall performance. To demonstrate the effectiveness of multi-task learning on failure diagnosis, we adopted the inter-task affinity [10] to measure the mutual effect between tasks. More concretely, given two tasks  $\mathcal{T}$  and  $\mathcal{T}'$ , the affinity  $Z_{\mathcal{T} \rightarrow \mathcal{T}'}$  can be approximated as the impact of  $\mathcal{T}$ 's gradient on the loss of  $\mathcal{T}'$ :

$$Z_{\mathcal{T} \rightarrow \mathcal{T}'} = 1 - \frac{\mathcal{L}_{\mathcal{T}'}(f, \theta_{s|\mathcal{T}}, \theta_{\mathcal{T}'})}{\mathcal{L}_{\mathcal{T}'}(f, \theta_s, \theta_{\mathcal{T}'}), \quad (21)}$$

where  $\theta_s$  and  $\theta_{\mathcal{T}'}$  denote the shared parameters of the two tasks and task  $\mathcal{T}'$ 's specific parameters, respectively. Given the fused feature  $f$ , we update the shared parameters  $\theta_{s|\mathcal{T}}$  by leveraging the gradient of task  $\mathcal{T}$  and the corresponding loss  $\mathcal{L}_{\mathcal{T}'}$ . According to [10], the affinity  $Z_{\mathcal{T} \rightarrow \mathcal{T}'}$  is positive when the gradient update of task  $\mathcal{T}$  leads to a lower loss of another task  $\mathcal{L}_{\mathcal{T}'}$ . Moreover, a higher absolute value of affinity  $Z_{\mathcal{T} \rightarrow \mathcal{T}'}$  indicates a greater impact of task  $\mathcal{T}$  on task  $\mathcal{T}'$ . We calculated the inter-task affinity at each step within a training epoch and outputted their mean.

**Results:** Fig. 13 shows the performance comparison of discarding modalities across two datasets. For dataset  $\mathcal{A}$ , the variants of *TVDiag* based on trace (*w/ Trace*) or metric (*w/ Metric*) achieve over 40% in  $HR@1$ , while the log-based variant (*w/ Log*) performs modestly in the RCL task but exhibits remarkable effectiveness in the FTI task. This suggests that diagnosis tasks favor specific modalities. On the dataset  $\mathcal{B}$ , the *w/ Log* performs slightly poorer than other modalities in terms of FTI, as most of the injected failures in dataset  $\mathcal{B}$  are resource-related, and the relevant information is recorded by the performance metrics but ignored by the logs. Therefore, FTI does not show a preference for incomplete logs on the dataset  $\mathcal{B}$ . It can be seen that the comprehensiveness of log information significantly affects the preference of FTI.

We further ablated one modality at a time to measure the impact of different modalities in *TVDiag*. Specifically, the lack of metrics (*w/o Metric*) or traces (*w/o Trace*) causes a significant decline in

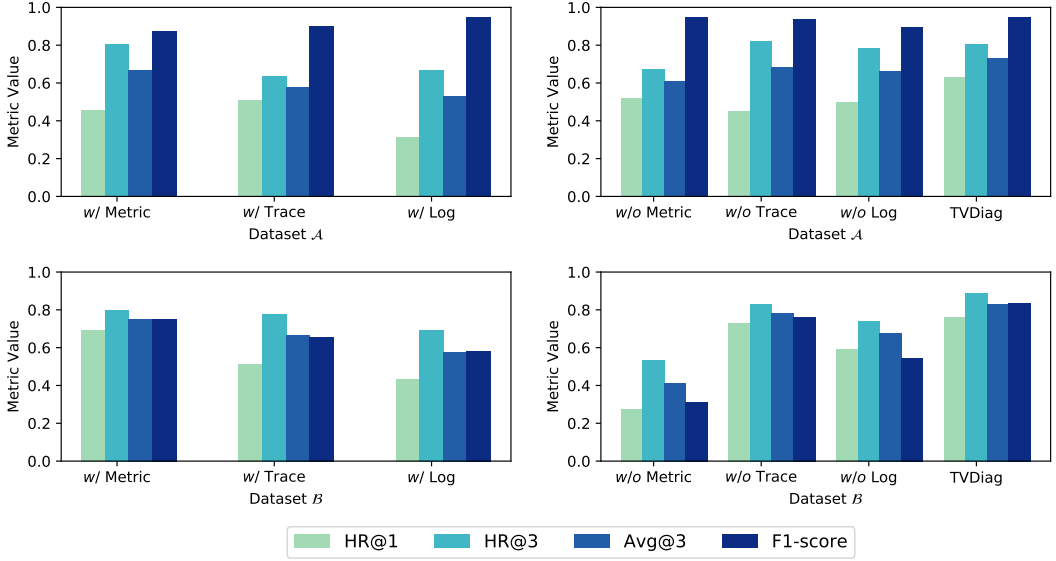


Fig. 13. Performance comparison of discarding different modalities.  $w/D$  represents a variant of  $TVDiag$  that only retains modality  $D$ , while  $w/o D$  is the variant which removes modality  $D$ .

Table 7. Inter-task affinity on two datasets.

Dataset	$\mathcal{A}$		$\mathcal{B}$	
	$Z_{RCL \rightarrow FTI}$	$Z_{FTI \rightarrow RCL}$	$Z_{RCL \rightarrow FTI}$	$Z_{FTI \rightarrow RCL}$
Affinity Value	$1.23 \times 10^{-1}$	$6.29 \times 10^{-3}$	$-5.11 \times 10^{-3}$	$3.58 \times 10^{-2}$

$HR@1$  (11.1% ~ 18.0%) in dataset  $\mathcal{A}$  but has little impact on F1-score. This finding validates the importance of metrics and traces in locating the root cause. On the other hand, the absence of logs ( $w/o$  Log) degrades the F1-score in identifying failure types (5.5% ~ 28.6%) across two datasets. Moreover, the degradation in  $HR@1$  also indicates that the alert information in logs contributes to the RCL task. The results indicate that the absence of a certain modality has varying impacts on the two diagnosis tasks.

Table 7 presents the inter-task affinity between RCL and FTI (i.e.,  $Z_{RCL \rightarrow FTI}$  and  $Z_{FTI \rightarrow RCL}$ ) for two datasets. The positive results suggest that the parameter updates from one task positively contribute to the learning of the other. In dataset  $\mathcal{A}$ ,  $Z_{RCL \rightarrow FTI}$  and  $Z_{FTI \rightarrow RCL}$  both are positive, indicating that the two tasks have a complementary relationship during the training process. Although the  $Z_{RCL \rightarrow FTI}$  in dataset  $\mathcal{B}$  is negative, the higher  $Z_{FTI \rightarrow RCL}$  prompts us to still opt for the fusion of the two tasks. Therefore, we can reasonably speculate that these two diagnosis tasks share certain related features, thereby gaining increased attention in multi-task learning.

**Answer to RQ4:** The absence of one or more observability modalities inevitably impairs the diagnostic performance. The experimental results of single-modal methods indicate that diagnostic tasks exhibit a bias towards specific modalities; e.g., the RCL task leans towards metrics and traces, while the FTI task favors logs. Furthermore, the combination of the RCL

and FTI tasks manifests a strong inter-task affinity, ensuring the plausibility of joint learning of these two diagnostic tasks.

## 5.6 Threats to Validity

The *internal threat to validity* concerns the bias and repeatability of experimental results. The major threat to internal validity lies in the implementation of *TVDiag* and other competing methods. For the RCL task, because Eadro did not publish the preprocessing code, we independently completed the data preprocessing steps introduced in [23] and applied them consistently to the two open datasets. Additionally, we rigorously reproduced the essential modules like log parsing while keeping the main model unchanged. DiagFusion [68], MicroRCA [58], and MicroRank [62] have released their complete code, enabling us to directly utilize them for reproducibility assurance. For the FTI task, LogCluster [33] also has not released the corresponding source code. To mitigate this threat, we strive to replicate the techniques exactly as described in the original paper, such as log parsing and log clustering. In terms of *TVDiag*, we implemented data augmentation, contrastive loss, and automatic weight adjustment using widely used open-source code to reduce the risk of invalidity. The overall architecture of *TVDiag* was also established based on prevalent frameworks such as PyTorch, scikit-learn, and DGL. To guarantee the reproducibility of our method, we fixed the random seed and preserved the intermediate alert features during experiments.

The *external threat to validity* is primarily related to the generalizability of our proposed method. One major external threat is the limited size of labeled data in the two datasets. In particular, there are only 113 records of failure injection in the original AIOps-22 dataset. To mitigate this threat, we expanded the dataset with a sliding window for each failure record and further performed a data augmentation strategy. Another external threat is the uncertain data quality of logs, given the significant variations in log standards among microservice-based systems. The logs of the GAIA dataset contain rich events at both software and hardware levels, whereas the log information in AIOps-22 is more limited. This variability can directly impact task-oriented learning in *TVDiag*. How to automatically select appropriate diagnosis tasks for guidance in task-oriented learning according to the contents of logs remains a part of our future work.

Although the two datasets mentioned above may not represent all online microservices systems, we believe *TVDiag* is sufficiently robust to perform well in most scenarios. This is because the input multimodal monitoring data is consistent in terms of data models, even across different microservice-based systems. For example, trace data mainly adhere to the specifications of OpenTracing [43] or OpenTelemetry [11]. Metrics are typically recorded at fixed time intervals in time-series databases [60]. Logs are also derived from a small number of templates. These data can be easily transformed into unified alerts with the methods described in Section § 4.1.

## 6 RELATED WORK

In a microservice-based system, a simple failure in one microservice may prevent the overall system from running normally and seriously affect the user experience [15, 54]. Recently, numerous failure diagnosis methods have been proposed to locate the root cause and identify the failure type.

### 6.1 Single-modal Failure Diagnosis

Existing single-modal failure diagnosis methods can be categorized into three types according to the dependent modality [68]: metric-based, trace-based, and log-based approaches.

**Metric-based approaches** [6, 20, 30, 32, 38, 39, 50, 56–58, 70]. Metrics record the running status and performance of a microservice-based system in the form of time series data. Many approaches

[6, 32, 40] attempt to construct causal relationships between microservices through metrics and infer the root cause based on simple backtracking. For example, MicroCause [40] builds a causal dependency graph based on collected metrics and performs a random walk to locate the root cause. However, these causal-based methods often construct certain spurious relationships due to the interference of data noise. To overcome this limitation, many methods [20, 29, 30] use deep learning to exploit the hidden metrics information. For instance, DejaVu [30] extracts the temporal features of metrics with recurrent neural networks, aggregates them in a failure dependency graph, and finally scores all components to filter out the root cause and identify the failure type. However, the failure dependency graph requires engineers to build in advance based on their own experience.

**Trace-based approaches** [15, 27, 28, 41, 48, 62, 65, 72]. Traces record the invocation details between microservices, which plays an indispensable role in reproducing the internal correlations of a microservice-based system. Numerous studies focus on extracting the critical path of failures by tracing the correlation between microservices [15, 28, 62]. For example, MicroRank [62] establishes a microservice correlation graph from traces and analyzes root causes by combining spectrum analysis and the PageRank algorithm. In contrast, MEPFL [72] directly performs supervised classification on traces of failures, achieving good performance as well.

**Log-based approaches** [1, 2, 9, 12, 19, 26, 44, 49, 66]. Logs are a primary source for diagnosing failures and debugging faults in microservice-based systems. Various log-based failure diagnosis techniques have been proposed, leveraging classical machine learning and deep learning approaches. For example, DyCause [44] combines API logs from multiple applications based on the crowdsourcing strategy to locate the root cause. However, DyCause only leverages the response time recorded in API logs. DeepLog [9], on the other hand, parses logs and extracts features to predict the next log, enabling the timely detection of abnormal logs.

Single-modal methods are limited in their ability to observe only the restricted information provided by a single view, which makes it challenging to diagnose certain failures that are only apparent in other views.

## 6.2 Multimodal Failure Diagnosis

In recent years, the fusion of multimodal monitoring data has gained attention in the field of anomaly detection [24, 67, 71]. Researchers have also shown interest in integrating the advantages of different modalities to further improve the performance of failure diagnosis [14, 17, 21, 42, 55, 64]. For instance, Wang et al. [55] enhanced metric-based RCL by incorporating log anomaly detection. Nezha [64] extracts event patterns from heterogeneous multimodal data, fostering the interpretability of RCL results by comparing normal and abnormal patterns. However, its fusion of logs and traces requires invasive configuration, which may not be applicable to all systems. In addition, several studies leverage deep learning to mine and fuse the latent information of the three modalities. DiagFusion [68], for example, fuses all modalities during data preparation by unifying them into events, which are then encoded as features for downstream diagnostic tasks. DiagFusion adopts an early fusion strategy to provide unified information from heterogeneous modalities, reducing the complexity of data processing. In contrast, Eadro [23] concatenates the representation of each modality during model training. This intermediate fusion can integrate high-dimensional knowledge from all modalities to improve overall performance.

Both approaches directly fuse the multimodal data, which may hardly capture the underlying associations among various modalities and neglect the potential relationship between diagnosis tasks and modalities. To address this limitation, we combine the strengths of the above two state-of-the-art approaches by fusing high-dimensional graph-level features of alerts from three modalities. Our *TVDiag* designs a modality-specific feature learning method based on task-oriented learning and constructs cross-modal associations to fully exploit the potential contribution of each modality.

## 7 CONCLUSION AND FUTURE WORK

This paper presents *TVDiag*, a multimodal failure diagnosis framework that integrates task-oriented learning and cross-modal association to locate the root causes and identify the type of failures in microservice-based systems. To fully leverage the potential of each modality in corresponding tasks, *TVDiag* employs a novel task-oriented learning method by maximizing the commonality between training samples belonging to the specific modality with the same failure type. Unlike previous multimodal diagnosis methods that ignore the view-invariant information among modalities, *TVDiag* incorporates a cross-modal association method based on contrastive learning to reinforce the view-invariant failure information. Furthermore, *TVDiag* randomly inactivates non-root cause instances to augment the training data, mitigating the issue of insufficient labeled data and incorporating failure scenarios with incomplete observability. Extensive experimental results demonstrate the effectiveness of *TVDiag* in both root cause localization and failure type identification.

In the future, we will explore additional combinations of diagnosis tasks in *TVDiag*, such as anomaly detection and failure prediction. Furthermore, we plan to investigate how to automate task-oriented learning rather than manually designate the relationship between tasks and modalities.

## ACKNOWLEDGMENTS

This work is supported by the National Key Research and Development Program of China (No. 2022YFF0902701) and the National Natural Science Foundation of China (No. 62032016).

## REFERENCES

- [1] Anunay Amar and Peter C Rigby. 2019. Mining historical test logs to predict bugs and localize faults in the test logs. In *2019 IEEE/ACM 41st International Conference on Software Engineering (ICSE)*. IEEE, 140–151.
- [2] Chetan Bansal, Sundararajan Renganathan, Ashima Asudani, Olivier Midy, and Mathru Janakiraman. 2020. Decaf: Diagnosing and triaging performance issues in large-scale cloud services. In *Proceedings of the ACM/IEEE 42nd International Conference on Software Engineering: Software Engineering in Practice*. 201–210.
- [3] Stephen J. Bigelow. 2022. What is observability? A beginner’s guide. <https://www.techtarget.com/searchitoperations/definition/observability/>.
- [4] Piotr Bojanowski, Edouard Grave, Armand Joulin, and Tomas Mikolov. 2017. Enriching word vectors with subword information. *Transactions of the association for computational linguistics* 5 (2017), 135–146.
- [5] Long Chen, Fei Wang, Ruijing Yang, Fei Xie, Wenjing Wang, Cai Xu, Wei Zhao, and Ziyu Guan. 2022. Representation learning from noisy user-tagged data for sentiment classification. *International Journal of Machine Learning and Cybernetics* 13, 12 (2022), 3727–3742.
- [6] Pengfei Chen, Yong Qi, and Di Hou. 2016. CauseInfer: Automated end-to-end performance diagnosis with hierarchical causality graph in cloud environment. *IEEE transactions on services computing* 12, 2 (2016), 214–230.
- [7] Ting Chen, Simon Kornblith, Mohammad Norouzi, and Geoffrey Hinton. 2020. A simple framework for contrastive learning of visual representations. In *International conference on machine learning*. PMLR, 1597–1607.
- [8] Min Du and Feifei Li. 2018. Spell: Online streaming parsing of large unstructured system logs. *IEEE Transactions on Knowledge and Data Engineering* 31, 11 (2018), 2213–2227.
- [9] Min Du, Feifei Li, Guineng Zheng, and Vivek Srikumar. 2017. Deeplog: Anomaly detection and diagnosis from system logs through deep learning. In *Proceedings of the 2017 ACM SIGSAC conference on computer and communications security*. 1285–1298.
- [10] Chris Fifty, Ehsan Amid, Zhe Zhao, Tianhe Yu, Rohan Anil, and Chelsea Finn. 2021. Efficiently identifying task groupings for multi-task learning. *Advances in Neural Information Processing Systems* 34 (2021), 27503–27516.
- [11] C. N. C. Foundation. 2024. OpenTelemetry. <https://opentelemetry.io/docs/concepts/sampling/>.
- [12] Xiaoyu Fu, Rui Ren, Sally A McKee, Jianfeng Zhan, and Ninghui Sun. 2014. Digging deeper into cluster system logs for failure prediction and root cause diagnosis. In *2014 IEEE International Conference on Cluster Computing (CLUSTER)*. IEEE, 103–112.
- [13] Google. 2024. [Online]. Available. <https://github.com/GoogleCloudPlatform/microservices-demo>.
- [14] Shenghui Gu, Guoping Rong, Tian Ren, He Zhang, Haifeng Shen, Yongda Yu, Xian Li, Jian Ouyang, and Chunhan Chen. 2023. TrinityRCL: Multi-Granular and Code-Level Root Cause Localization Using Multiple Types of Telemetry Data in Microservice Systems. *IEEE Transactions on Software Engineering* (2023).

[15] Xiaofeng Guo, Xin Peng, Hanzhang Wang, Wanxue Li, Huai Jiang, Dan Ding, Tao Xie, and Liangfei Su. 2020. Graph-based trace analysis for microservice architecture understanding and problem diagnosis. In *Proceedings of the 28th ACM Joint Meeting on European Software Engineering Conference and Symposium on the Foundations of Software Engineering*. 1387–1397.

[16] Will Hamilton, Zhitao Ying, and Jure Leskovec. 2017. Inductive representation learning on large graphs. *Advances in neural information processing systems* 30 (2017).

[17] Jingzhu He, Yuhang Lin, Xiaohui Gu, Chin-Chia Michael Yeh, and Zhongfang Zhuang. 2022. PerfSig: extracting performance bug signatures via multi-modality causal analysis. In *Proceedings of the 44th International Conference on Software Engineering*. 1669–1680.

[18] Pinjia He, Jieming Zhu, Zibin Zheng, and Michael R Lyu. 2017. Drain: An online log parsing approach with fixed depth tree. In *2017 IEEE international conference on web services (ICWS)*. IEEE, 33–40.

[19] Shilin He, Qingwei Lin, Jian-Guang Lou, Hongyu Zhang, Michael R Lyu, and Dongmei Zhang. 2018. Identifying impactful service system problems via log analysis. In *Proceedings of the 2018 26th ACM Joint Meeting on European Software Engineering Conference and Symposium on the Foundations of Software Engineering*. 60–70.

[20] Zilong He, Pengfei Chen, Yu Luo, Qiuyu Yan, Hongyang Chen, Guangba Yu, and Fangyuan Li. 2022. Graph based Incident Extraction and Diagnosis in Large-Scale Online Systems. In *37th IEEE/ACM International Conference on Automated Software Engineering*. 1–13.

[21] Chuanjia Hou, Tong Jia, Yifan Wu, Ying Li, and Jing Han. 2021. Diagnosing Performance Issues in Microservices with Heterogeneous Data Source. In *2021 IEEE Intl Conf on Parallel & Distributed Processing with Applications, Big Data & Cloud Computing, Sustainable Computing & Communications, Social Computing & Networking (ISPA/BDCloud/SocialCom/SustainCom)*. IEEE, 493–500.

[22] Prannay Khosla, Piotr Teterwak, Chen Wang, Aaron Sarna, Yonglong Tian, Phillip Isola, Aaron Maschinot, Ce Liu, and Dilip Krishnan. 2020. Supervised contrastive learning. *Advances in neural information processing systems* 33 (2020), 18661–18673.

[23] Cheryl Lee, Tianyi Yang, Zhuangbin Chen, Yuxin Su, and Michael R Lyu. 2023. Eadro: An End-to-End Troubleshooting Framework for Microservices on Multi-source Data. *arXiv preprint arXiv:2302.05092* (2023).

[24] Cheryl Lee, Tianyi Yang, Zhuangbin Chen, Yuxin Su, Yongqiang Yang, and Michael R Lyu. 2023. Heterogeneous Anomaly Detection for Software Systems via Semi-supervised Cross-modal Attention. *arXiv preprint arXiv:2302.06914* (2023).

[25] Bowen Li, Xin Peng, Qilin Xiang, Hanzhang Wang, Tao Xie, Jun Sun, and Xuanzhe Liu. 2022. Enjoy your observability: an industrial survey of microservice tracing and analysis. *Empirical Software Engineering* 27 (2022), 1–28.

[26] Xiaoyun Li, Pengfei Chen, Linxiao Jing, Zilong He, and Guangba Yu. 2020. Swisslog: Robust and unified deep learning based log anomaly detection for diverse faults. In *2020 IEEE 31st International Symposium on Software Reliability Engineering (ISSRE)*. IEEE, 92–103.

[27] Yufeng Li, Guangba Yu, Pengfei Chen, Chuanfu Zhang, and Zibin Zheng. 2022. MicroSketch: Lightweight and Adaptive Sketch Based Performance Issue Detection and Localization in Microservice Systems. In *Service-Oriented Computing: 20th International Conference, ICSOC 2022, Seville, Spain, November 29–December 2, 2022, Proceedings*. Springer, 219–236.

[28] Zeyan Li, Junjie Chen, Rui Jiao, Nengwen Zhao, Zhijun Wang, Shuwei Zhang, Yanjun Wu, Long Jiang, Leiqin Yan, Zikai Wang, et al. 2021. Practical root cause localization for microservice systems via trace analysis. In *2021 IEEE/ACM 29th International Symposium on Quality of Service (IWQOS)*. IEEE, 1–10.

[29] Zhongliang Li, Yaofeng Tu, and Zongmin Ma. 2022. Root Cause Analysis of Anomalies Based on Graph Convolutional Neural Network. *International Journal of Software Engineering and Knowledge Engineering* 32, 08 (2022), 1155–1177.

[30] Zeyan Li, Nengwen Zhao, Mingjie Li, Xianglin Lu, Lixin Wang, Dongdong Chang, Xiaohui Nie, Li Cao, Wench Zhang, Kaixin Sui, et al. 2022. Actionable and interpretable fault localization for recurring failures in online service systems. In *Proceedings of the 30th ACM Joint European Software Engineering Conference and Symposium on the Foundations of Software Engineering*. 996–1008.

[31] Lukas Liebel and Marco Körner. 2018. Auxiliary tasks in multi-task learning. *arXiv preprint arXiv:1805.06334* (2018).

[32] JinJin Lin, Pengfei Chen, and Zibin Zheng. 2018. Microscope: Pinpoint performance issues with causal graphs in micro-service environments. In *Service-Oriented Computing: 16th International Conference, ICSOC 2018, Hangzhou, China, November 12–15, 2018, Proceedings 16*. Springer, 3–20.

[33] Qingwei Lin, Hongyu Zhang, Jian-Guang Lou, Yu Zhang, and Xuewei Chen. 2016. Log clustering based problem identification for online service systems. In *Proceedings of the 38th International Conference on Software Engineering Companion*. 102–111.

[34] Bingqian Liu, Duantengchuan Li, Jian Wang, Zhihao Wang, Bing Li, and Cheng Zeng. 2024. Integrating user short-term intentions and long-term preferences in heterogeneous hypergraph networks for sequential recommendation. *Information Processing & Management* 61, 3 (2024), 103680.

[35] Dewe Liu, Chuan He, Xin Peng, Fan Lin, Chenxi Zhang, Shengfang Gong, Ziang Li, Jiayu Ou, and Zheshun Wu. 2021. Microhecl: High-efficient root cause localization in large-scale microservice systems. In *2021 IEEE/ACM 43rd International Conference on Software Engineering: Software Engineering in Practice (ICSE-SEIP)*. IEEE, 338–347.

[36] Fei Tony Liu, Kai Ming Ting, and Zhi-Hua Zhou. 2008. Isolation forest. In *2008 eighth ieee international conference on data mining*. IEEE, 413–422.

[37] Jay Livens. 2023. What is observability? Not just logs, metrics and traces. <https://www.dynatrace.com/news/blog/what-is-observability-2/>.

[38] Meng Ma, Weilan Lin, Disheng Pan, and Ping Wang. 2020. Self-adaptive root cause diagnosis for large-scale microservice architecture. *IEEE Transactions on Services Computing* 15, 3 (2020), 1399–1410.

[39] Meng Ma, Jingmin Xu, Yuan Wang, Pengfei Chen, Zonghua Zhang, and Ping Wang. 2020. Automap: Diagnose your microservice-based web applications automatically. In *Proceedings of The Web Conference 2020*. 246–258.

[40] Yuan Meng, Shenglin Zhang, Yongqian Sun, Ruru Zhang, Zhilong Hu, Yiyin Zhang, Chenyang Jia, Zhaogang Wang, and Dan Pei. 2020. Localizing failure root causes in a microservice through causality inference. In *2020 IEEE/ACM 28th International Symposium on Quality of Service (IWQoS)*. IEEE, 1–10.

[41] Haibo Mi, Huaimin Wang, Yangfan Zhou, Michael Rung-Tsong Lyu, and Hua Cai. 2013. Toward fine-grained, unsupervised, scalable performance diagnosis for production cloud computing systems. *IEEE Transactions on Parallel and Distributed Systems* 24, 6 (2013), 1245–1255.

[42] Sasho Nedelkoski, Jasmin Bogatinovski, Ajay Kumar Mandapati, Soeren Becker, Jorge Cardoso, and Odej Kao. 2020. Multi-source distributed system data for ai-powered analytics. In *Service-Oriented and Cloud Computing: 8th IFIP WG 2.14 European Conference, ESOCC 2020, Heraklion, Crete, Greece, September 28–30, 2020, Proceedings 8*. Springer, 161–176.

[43] OpenTracing. 2024. OpenTracing. <https://opentracing.io/specification>.

[44] Yicheng Pan, Meng Ma, Xinrui Jiang, and Ping Wang. 2021. Faster, deeper, easier: crowdsourcing diagnosis of microservice kernel failure from user space. In *Proceedings of the 30th ACM SIGSOFT International Symposium on Software Testing and Analysis*. 646–657.

[45] Xin Peng, Chenxi Zhang, Zhongyuan Zhao, Akasaka Isami, Xiaofeng Guo, and Yunna Cui. 2022. Trace analysis based microservice architecture measurement. In *Proceedings of the 30th ACM Joint European Software Engineering Conference and Symposium on the Foundations of Software Engineering*. 1589–1599.

[46] Friedrich Pukelsheim. 1994. The three sigma rule. *The American Statistician* 48, 2 (1994), 88–91.

[47] Haoran Qiu, Subho S Banerjee, Saurabh Jha, Zbigniew T Kalbarczyk, and Ravishankar K Iyer. 2020. FIRM: An intelligent fine-grained resource management framework for slo-oriented microservices. In *Proceedings of The 14th USENIX Symposium on Operating Systems Design and Implementation (OSDI ’20)*.

[48] Jesus Rios, Saurabh Jha, and Laura Shwartz. 2022. Localizing and Explaining Faults in Microservices Using Distributed Tracing. In *2022 IEEE 15th International Conference on Cloud Computing (CLOUD)*. IEEE, 489–499.

[49] Carl Martin Rosenberg and Leon Moonen. 2020. Spectrum-based log diagnosis. In *Proceedings of the 14th ACM/IEEE International Symposium on Empirical Software Engineering and Measurement (ESEM)*. 1–12.

[50] Huasong Shan, Yuan Chen, Haifeng Liu, Yunpeng Zhang, Xiao Xiao, Xiaofeng He, Min Li, and Wei Ding. 2019. ?-diagnosis: Unsupervised and real-time diagnosis of small-window long-tail latency in large-scale microservice platforms. In *The World Wide Web Conference*. 3215–3222.

[51] Yicheng Sui, Yuzhe Zhang, Jianjun Sun, Ting Xu, Shenglin Zhang, Zhengdan Li, Yongqian Sun, Fangrui Guo, Junyu Shen, Yuzhi Zhang, et al. 2023. LogKG: Log Failure Diagnosis through Knowledge Graph. *IEEE Transactions on Services Computing* (2023).

[52] TVDiag. 2024. [Online]. Available. <https://github.com/WHU-AISE/TVDiag>.

[53] Feng Wang and Huaping Liu. 2021. Understanding the behaviour of contrastive loss. In *Proceedings of the IEEE/CVF conference on computer vision and pattern recognition*. 2495–2504.

[54] Lu Wang, Yu Xuan Jiang, Zhan Wang, Qi En Huo, Jie Dai, Sheng Long Xie, Rui Li, Ming Tao Feng, Yue Shen Xu, and Zhi Ping Jiang. 2022. The operation and maintenance governance of microservices architecture systems: A systematic literature review. *Journal of Software: Evolution and Process* (2022), e2433.

[55] Lingzhi Wang, Nengwen Zhao, Junjie Chen, Pinnong Li, Wench Zhang, and Kaixin Sui. 2020. Root-cause metric location for microservice systems via log anomaly detection. In *2020 IEEE International Conference on Web Services (ICWS)*. IEEE, 142–150.

[56] Canhua Wu, Nengwen Zhao, Lixin Wang, Xiaoqin Yang, Shining Li, Ming Zhang, Xing Jin, Xidao Wen, Xiaohui Nie, Wench Zhang, et al. 2021. Identifying root-cause metrics for incident diagnosis in online service systems. In *2021 IEEE 32nd International Symposium on Software Reliability Engineering (ISSRE)*. IEEE, 91–102.

[57] Li Wu, Johan Tordsson, Jasmin Bogatinovski, Erik Elmroth, and Odej Kao. 2021. Microdiag: Fine-grained performance diagnosis for microservice systems. In *2021 IEEE/ACM International Workshop on Cloud Intelligence (CloudIntelligence)*. IEEE, 31–36.

- [58] Li Wu, Johan Tordsson, Erik Elmroth, and Odej Kao. 2020. Microrca: Root cause localization of performance issues in microservices. In *NOMS 2020-2020 IEEE/IFIP Network Operations and Management Symposium*. IEEE, 1–9.
- [59] Ru Xie, Jing Yang, Jingying Li, and Liming Wang. 2023. ImpactTracer: Root Cause Localization in Microservices Based on Fault Propagation Modeling. In *2023 Design, Automation & Test in Europe Conference & Exhibition (DATE)*. IEEE, 1–6.
- [60] Shuaiyu Xie, Jian Wang, Bing Li, Zekun Zhang, Duantengchuan Li, and Patrick CK Hung. 2024. PBScaler: A Bottleneck-aware Autoscaling Framework for Microservice-based Applications. *IEEE Transactions on Services Computing* (2024).
- [61] Yuning You, Tianlong Chen, Yongduo Sui, Ting Chen, Zhangyang Wang, and Yang Shen. 2020. Graph contrastive learning with augmentations. *Advances in neural information processing systems* 33 (2020), 5812–5823.
- [62] Guangba Yu, Pengfei Chen, Hongyang Chen, Zijie Guan, Zicheng Huang, Linxiao Jing, Tianjun Weng, Xinnmeng Sun, and Xiaoyun Li. 2021. Microrank: End-to-end latency issue localization with extended spectrum analysis in microservice environments. In *Proceedings of the Web Conference 2021*. 3087–3098.
- [63] Guangba Yu, Pengfei Chen, Pairui Li, Tianjun Weng, Haibing Zheng, Yuetang Deng, and Zibin Zheng. 2023. Logreducer: Identify and reduce log hotspots in kernel on the fly. In *2023 IEEE/ACM 45th International Conference on Software Engineering (ICSE)*. IEEE, 1763–1775.
- [64] Guangba Yu, Pengfei Chen, Yufeng Li, Hongyang Chen, Xiaoyun Li, and Zibin Zheng. 2023. Nezha: Interpretable Fine-Grained Root Causes Analysis for Microservices on Multi-modal Observability Data. In *Proceedings of the 31st ACM Joint European Software Engineering Conference and Symposium on the Foundations of Software Engineering*. 553–565.
- [65] Guangba Yu, Zicheng Huang, and Pengfei Chen. 2021. TraceRank: Abnormal service localization with dis-aggregated end-to-end tracing data in cloud native systems. *Journal of Software: Evolution and Process* (2021), e2413.
- [66] Yue Yuan, Wenchang Shi, Bin Liang, and Bo Qin. 2019. An approach to cloud execution failure diagnosis based on exception logs in openstack. In *2019 IEEE 12th International Conference on Cloud Computing (CLOUD)*. IEEE, 124–131.
- [67] Chenxi Zhang, Xin Peng, Chaofeng Sha, Ke Zhang, Zhenqing Fu, Xiya Wu, Qingwei Lin, and Dongmei Zhang. 2022. DeepTraLog: Trace-log combined microservice anomaly detection through graph-based deep learning. In *Proceedings of the 44th International Conference on Software Engineering*. 623–634.
- [68] Shenglin Zhang, Pengxiang Jin, Zihan Lin, Yongqian Sun, Bicheng Zhang, Sibo Xia, Zhengdan Li, Zhenyu Zhong, Minghua Ma, Wa Jin, et al. 2023. Robust Failure Diagnosis of Microservice System through Multimodal Data. *arXiv preprint arXiv:2302.10512* (2023).
- [69] Shenglin Zhang, Zhongjie Pan, Heng Liu, Pengxiang Jin, Yongqian Sun, Qianyu Ouyang, Jiaju Wang, Xueying Jia, Yuzhi Zhang, Hui Yang, et al. 2023. Efficient and Robust Trace Anomaly Detection for Large-Scale Microservice Systems. In *2023 IEEE 34th International Symposium on Software Reliability Engineering (ISSRE)*. IEEE, 69–79.
- [70] Zekun Zhang, Bing Li, Jian Wang, and Yongqiang Liu. 2021. AAMR: Automated Anomalous Microservice Ranking in Cloud-Native Environment. (2021).
- [71] Nengwen Zhao, Junjie Chen, Zhaoyang Yu, Honglin Wang, Jiesong Li, Bin Qiu, Hongyu Xu, Wenchi Zhang, Kaixin Sui, and Dan Pei. 2021. Identifying bad software changes via multimodal anomaly detection for online service systems. In *Proceedings of the 29th ACM Joint Meeting on European Software Engineering Conference and Symposium on the Foundations of Software Engineering*. 527–539.
- [72] Xiang Zhou, Xin Peng, Tao Xie, Jun Sun, Chao Ji, Dewei Liu, Qilin Xiang, and Chuan He. 2019. Latent error prediction and fault localization for microservice applications by learning from system trace logs. In *Proceedings of the 2019 27th ACM Joint Meeting on European Software Engineering Conference and Symposium on the Foundations of Software Engineering*. 683–694.